



Palladium-catalyzed reaction of γ -silylated allyl acetates proceeding through 1,2-shift of a substituent on silicon

Yoshikazu Horino ^{a,*}, Mayo Ishibashi ^a, Kosuke Nakasai ^a, Toshinobu Korenaga ^{b,**}

^a Department of Environmental Applied Chemistry, Faculty of Engineering, University of Toyama, Toyama, 930-8555, Japan

^b Department of Chemistry and Bioengineering, Faculty of Engineering, Iwate University, Morioka, Iwate, 020-8551, Japan

ARTICLE INFO

Article history:

Received 4 April 2020

Received in revised form

7 August 2020

Accepted 8 August 2020

Available online 16 August 2020

Keywords:

π -Allylpalladium

Migration

Palladium

Allylsilanes

Homoallylic alcohols

ABSTRACT

The palladium-catalyzed reaction of γ -silylated allyl acetates with water in the presence of CsF induces a previously unprecedented 1,2-shift of a substituent on silicon to produce allylsilanes in situ. The catalytic activity of the palladium increased when using an electron-poor phosphine ligand possessing fluorinated substituents. Further investigation of the reaction revealed that the approximate order of the migratory aptitude of groups from silicon was $\text{PhC}\equiv\text{C}$, allyl > Bn > Ph, vinyl > alkyl (Me, Et). A density functional theory study was employed to explore the reaction mechanism. Finally, the Hosomi–Sakurai-type allylation of aldehydes with in situ-generated α,γ -disubstituted allylsilanes was also investigated.

© 2020 Elsevier Ltd. All rights reserved.

1. Introduction

Due to their increased Lewis acidity at silicon atom and enhanced Si–C bond reactivity, hypervalent organosilicate species constitute important key intermediates in organic synthesis and exhibit rich and diverse chemistry in carbon–carbon bond forming reactions [1–4]. For example, transition-metal-catalyzed cross-coupling reactions such as the Hiyama coupling reaction have emerged as particularly valuable synthetic tools because of the many attractive properties of organosilanes, such as ease of preparation, stability, and environmentally benign nature [5–7]. In another well-studied example—the Hosomi–Sakurai reaction—the allylation of carbonyl groups with allylsilanes proceeds stereoselectively with high functional group tolerance, compared with other organometallic reagents of the main-group elements [8–14]. Recently, the defluoroallylation of trifluoromethylarenes with allylsilanes was reported by the Bandar group, wherein a fluoride-anion-induced single-electron-transfer pathway was responsible for the C–F substitution event [15]. In contrast, there are few reports on π -allylpalladium-mediated carbon–carbon

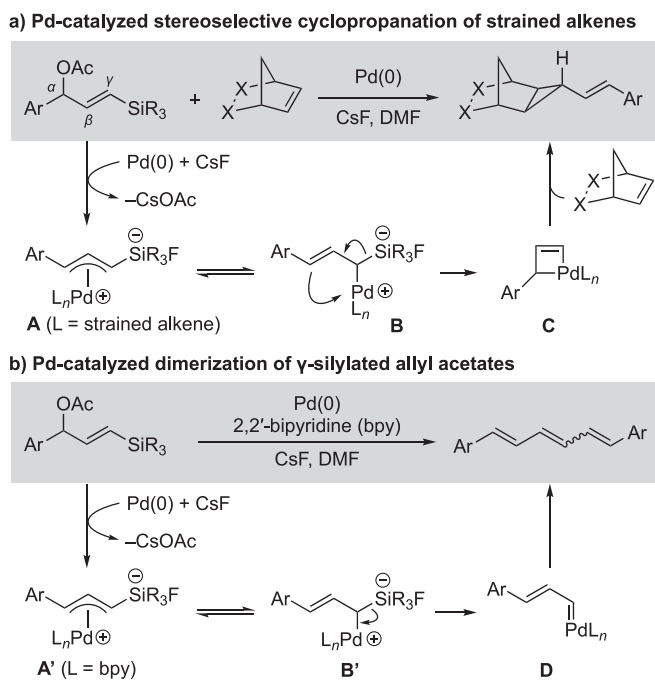
bond forming reactions with organosilanes, although the π -allylpalladium-mediated reaction has been widely studied in a large number of important organic transformations [16,17]. In this context, DeShong et al. developed the palladium-catalyzed phenylation of allylic benzoates using tetrabutylammonium triphenyldifluorosilicate (TBAT) as a hypervalent silicate [18–23]. Although TBAT is still a useful reagent—not only as a potent source of the fluoride anion [20,24,25] but also in palladium-catalyzed coupling reactions [23]—the lack of reports on the functional group-tolerant synthesis of TBAT derivatives [22] indicates that there is further need for alternative strategies in its application to carbon–carbon bond forming reactions.

We previously found that silyl-substituted π -allylpalladium intermediate **A**, generated from the palladium-catalyzed reaction of γ -silylated allylic acetates in the presence of CsF, exhibited unique reactivities other than simple allylation [26,27]. For example, we reported the stereoselective cyclopropanation of strained alkenes by the palladium-catalyzed reaction of γ -silylated allyl acetates, which was proposed to proceed via the formation of putative palladacyclobutene **C** from **B** (Scheme 1a) [26]. Furthermore, in the presence of the 2,2'-bipyridine ligand, palladium-stabilized vinylcarbene intermediate **D** was formed from **B'**, which underwent carbene dimerization (Scheme 1b) [27]. These examples indicate that an in situ-generated a cationic silylated π -allylpalladium intermediates **A** and **A'** (or a transient gem-silyl- σ -allylpalladium

* Corresponding author.

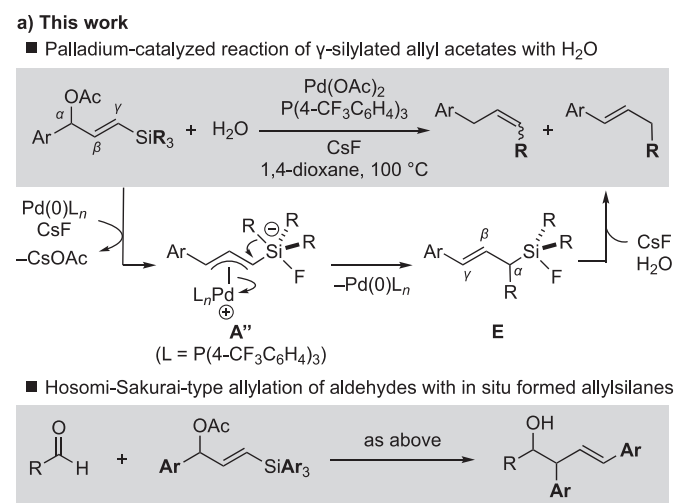
** Corresponding author.

E-mail addresses: horino@eng.u-toyama.ac.jp (Y. Horino), korenaga@iwate-u.ac.jp (T. Korenaga).

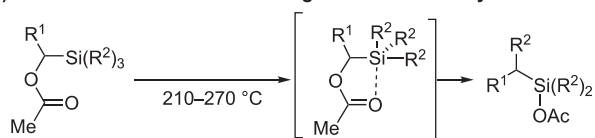


Scheme 1. Reactivities of silylated π -allylpalladium intermediates.

intermediate) play important roles in determining the reaction path. We envisioned that this concept could be extended to the generation of allylsilane **E** (Scheme 2a), wherein the intramolecular migration of a substituent on silicon to an allylic carbon in hypervalent organosilicate intermediate **A''** would be induced. In fact, Buynak et al. reported the thermal rearrangement of α -acetoxysilanes to silyl acetates, where intramolecular coordination between the silicon and carbonyl oxygen atoms was critical to promote the reaction (Scheme 2b) [28]. However, as synthetic



b) Previous work: Thermal rearrangement of α -acetoxysilanes



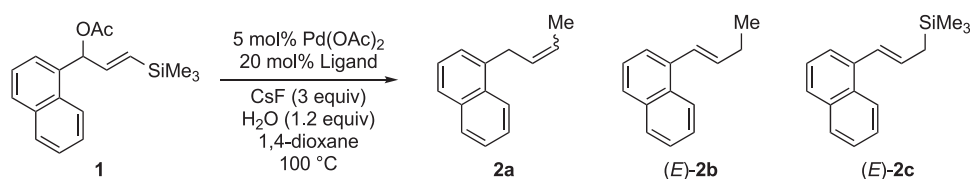
Scheme 2. 1,2-Shift of a substituent on silicon to carbon.

routes to acylsilanes as precursors for α -acetoxysilanes are limited [29,30], and high reaction temperatures are required for such rearrangements ($>210\text{ }^\circ\text{C}$), the thermal rearrangement of α -acetoxysilanes has not yet evolved as a practical and general synthetic method. Herein, we report the palladium-catalyzed reaction of γ -silylated allyl acetates with water, in which a previously unprecedented 1,2-shift of a substituent on silicon in the silylated π -allylpalladium intermediate is induced (Scheme 2a) [31–35]. Then, the Hosomi–Sakurai-type allylation of aldehydes with in situ-generated α,γ -disubstituted allylsilanes **E** was also examined.

2. Results

2.1. Optimization

Initially, we screened the palladium-catalyzed reaction of γ -trimethylsilyl-substituted allyl acetate **1** with water by evaluating various ligands (Table 1). The reaction of **1** (1 equiv) and H_2O (1.2 equiv) in the presence of $\text{Pd}(\text{OAc})_2$ (5 mol%), PPh_3 (20 mol%), and CsF (3 equiv) in 1,4-dioxane under an argon atmosphere at $100\text{ }^\circ\text{C}$ formed only an unexpected by-product, (E)-**2c** (entry 1). The reaction pathway leading to (E)-**2c** is not presently clear. In the presence of an electron-rich phosphine ligand such as $\text{P}(4\text{-MeOC}_6\text{H}_4)_3$, no conversion was observed, even though electron-rich phosphines are known to promote the palladium-catalyzed phenylation of allyl benzoates using TBAT (entry 2) [21]. These results suggest that the ligands decrease the electrophilicity of cationic π -allylpalladium intermediate **A''**, as shown in Scheme 2a. The efficiency of this transformation appears to be highly dependent on the electronic properties of the phosphine ligand. To our delight, the catalytic activity of palladium significantly improved when the ligand was changed to electron-poor phosphines possessing fluorinated substituents (entries 3–8). For example, the use of $\text{P}(4\text{-FC}_6\text{H}_4)_3$ produced **2a** and (E)-**2b** in 46% and 10% yields, respectively (entry 3). Further sequential improvements were observed upon switching to $\text{P}(4,5\text{-F}_2\text{C}_6\text{H}_3)_3$ (total 75%, entry 5), $\text{P}(3,4,5\text{-F}_3\text{C}_6\text{H}_2)_3$ (total 76%, entry 6), $\text{P}(4\text{-CF}_3\text{C}_6\text{H}_4)_3$ (total 76%, entry 7), and $\text{P}(3\text{-F-4-CF}_3\text{C}_6\text{H}_3)_3$ (total 71%, entry 8). Thus, electron-poor phosphine ligands possessing fluorinated substituents play a crucial role in the process of 1,2-shift. The reason that palladium complexes ligated by electron-poor phosphines favor 1,2-shift is that makes the palladium center more electrophilic. Accordingly, the resulting π -allylpalladium intermediate is susceptible to intramolecular nucleophilic attack from the substituent on silicon. It should be noted that phosphines with increased electron deficiency, such as $\text{P}(3,5\text{-F}_2\text{-4-CF}_3\text{C}_6\text{H}_2)_3$, $\text{P}[3,5\text{-(CF}_3)_2\text{C}_6\text{H}_3]_3$, $\text{P}(\text{C}_6\text{F}_5)_3$, or $\text{P}(\text{BFPy})_3$ [36,37] were not effective for this transformation (entries 9–12). The yield of the products was lower when the phosphine/palladium (P: Pd) ratio was 3:1 rather than 4:1 (entry 13). Based on these experiments, both $\text{P}(3,4,5\text{-F}_3\text{C}_6\text{H}_2)_3$ and $\text{P}(4\text{-CF}_3\text{C}_6\text{H}_4)_3$ were promising ligands. However, when $\text{P}(3,4,5\text{-F}_3\text{C}_6\text{H}_2)_3$ was applied in cases with heteroaryl-substituted silyl groups instead of a trimethylsilyl group, the transformation was not general, and broader evaluation identified $\text{P}(4\text{-CF}_3\text{C}_6\text{H}_4)_3$ as optimal. In addition, the catalyst loading could be reduced to 2.5 mol% without significant loss of catalytic activity when using $\text{P}(4\text{-CF}_3\text{C}_6\text{H}_4)_3$ (entry 14). Although the combination of CsF and 18-crown-6 is known to be effective for the generation of hypervalent silicates [15,25,38], the addition of 18-crown-6 failed to promote the present reaction (entry 15). Nevertheless, the reaction requires activation by the fluoride anion, as was shown by the absence of desired products when the reaction was performed without a fluoride anion source (entries 16 and 17). It is worth noting that use of TBAT instead of CsF promoted protodesilylation of **1** to give 1-(3-acetoxy-1-propen-1-yl)naphthalene in 55% yield (entry 18). In

Table 1
Optimization of reaction conditions.^a

entry	ligand	time (h)	2a (%)	E/Z	(E)- 2b (%)	(E)- 2c (%)
1	PPh ₃	12	0		0	7
2	P(4-MeOC ₆ H ₄) ₃	12	0		0	
3	P(4-FC ₆ H ₄) ₃	4.5	46	1:6.6	10	
4	P(3,5-F ₂ C ₆ H ₃) ₃	9	43	1:7	10	5
5	P(4,5-F ₂ C ₆ H ₃) ₃	4	58	1:7	17	
6	P(3,4,5-F ₃ C ₆ H ₂) ₃	5	60	1:7.2	16	
7	P(4-CF ₃ C ₆ H ₄) ₃	6	62	1:7.2	14	
8	P(3-F-4-CF ₃ C ₆ H ₃) ₃	6	57	1:7.1	14	2
9	P(3,5-F ₂ -4-CF ₃ C ₆ H ₂) ₃	11	15	1:8.6	3	5
10	P[3,5-(CF ₃) ₂ C ₆ H ₃] ₃	24	complex mixture			
11	P(C ₆ F ₅) ₃	12	0		0	
12 ^b	P(BFPy) ₃	12	0		0	
13 ^c	P(4-CF ₃ C ₆ H ₄) ₃	22	46	1:7.5	11	5
14 ^d	P(4-CF ₃ C ₆ H ₄) ₃	10	55	1:7.2	17	
15 ^e	P(4-CF ₃ C ₆ H ₄) ₃	12	0		0	
16 ^f	P(4-CF ₃ C ₆ H ₄) ₃	12	0		0	
17 ^g	P(4-CF ₃ C ₆ H ₄) ₃	12	0		0	
18 ^h	P(4-CF ₃ C ₆ H ₄) ₃	1	0		0	
19 ⁱ	—	12	0		0	
20 ^j	P(4-CF ₃ C ₆ H ₄) ₃	4.5	52	1:7.7	15	

^a Conditions: **1** (0.5 mmol), H₂O (0.6 mmol), Pd(OAc)₂ (5 mol%), ligand (20 mol%), CsF (1.5 mmol) in 1,4-dioxane (3 mL) at 100 °C.

^b P(BFPy)₃ = tris(2,6-bis(trifluoromethyl)-4-pyridyl)phosphine.

^c P(4-CF₃C₆H₄)₃ (7.5 mol%) was used.

^d Pd(OAc)₂ (2.5 mol%) and ligand (10 mol%) were used.

^e 18-crown-6 (0.9 mmol) was used.

^f CsOAc was used instead of CsF.

^g Reaction was performed in the absence of CsF.

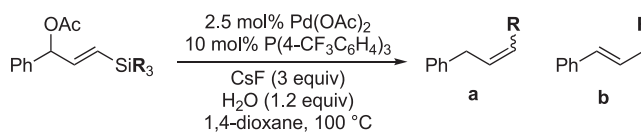
^h TBAT was used instead of CsF.

ⁱ Reaction was performed in the absence of Pd(OAc)₂ and ligand, and **1** was recovered in 98%.

^j Reaction was performed in the absence of H₂O.

addition, palladium-catalyzed phenylation of **1** with TBAT was not observed [18,20–23]. The reaction also failed in the absence of the Pd catalyst and **1** was recovered in 98% yield, proving that the formation of a π -allylpalladium intermediate plays an important role in the present process (entry 19). Finally, the reaction was examined in the absence of water, which is expected to intercept the in situ-generated allylsilane intermediates. ¹H NMR monitoring experiments before quenching the reaction mixture did not reveal the presence of allylsilane intermediates. Instead, **2a** and (**E**)-**2b** were obtained in 52% and 15% yields, respectively, likely due to the

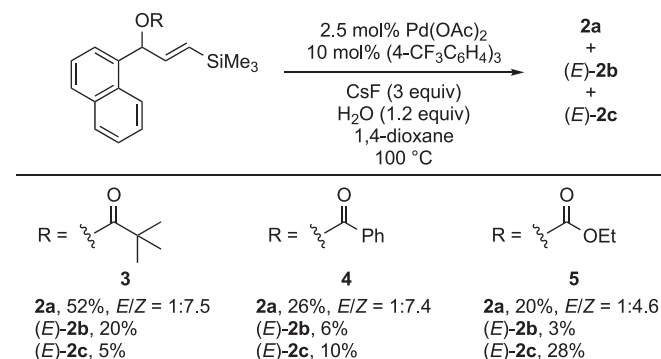
trace amounts of water contained in the solvent and CsF (entry 20). Although many efforts have been made to detect the allylsilane derivatives that would be expected in the absence of water, hydrolysis could not be avoided, probably because the hypervalent allylsilanes generated in our system are not sufficiently stable.

Table 2
Substrate scope.^a

entry	substrate (R)	time (h)	a (%)	E/Z	b (%)
1	6 (R = Ph)	6	7a : 76	17.5:1	
2	8 (R = 4-CF ₃ C ₆ H ₄)	3	9a : 28	20:1	9b : 58
3	10 (R = 4-MeOC ₆ H ₄)	11	11a : 51	3.2:1	11b : 33
4	12 (R = 2-furyl)	7	13a : 25	1:1	13b : 39
5	14 (R = 2-thienyl)	11	15a : 13	1.2:1	15b : 49
6	16 (R = Et)	12	17a : 33	1:3.3	17b : 15
7 ^b	18 (R = i-Pr)	24	19a : 0		19b : 0

^a Conditions: substrate (0.5 mmol), H₂O (0.6 mmol), Pd(OAc)₂ (2.5 mol%), P(4-CF₃C₆H₄)₃ (10 mol%), CsF (1.5 mmol) in 1,4-dioxane (3 mL) at 100 °C.

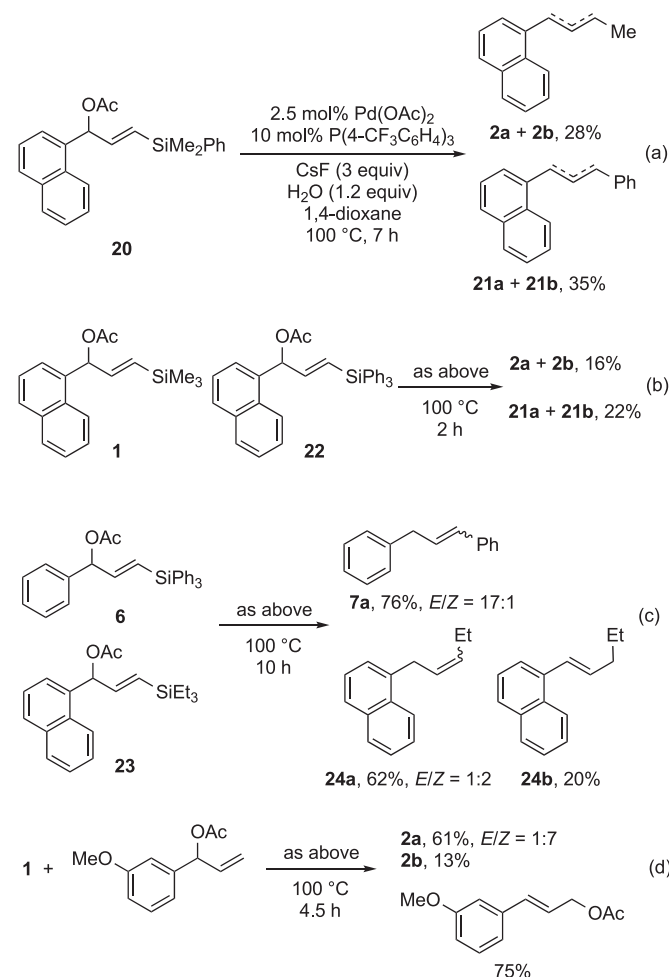
^b **18** was recovered in 78% isolated yield.

**Scheme 3.** Effect of leaving group on the efficiency of the 1,2-shift of methyl group from silicon to carbon.

Interestingly, it was found that the identity of the leaving group also has an influence on the 1,2-shift of a methyl group from silicon to carbon (Scheme 3). The reaction of **3** bearing a pivaloyloxy group instead of an acetoxy group exhibited similar reactivity in the model reaction compared with **1** (Table 1, entry 14), affording desired products **2a** and (E)-**2b** in 52% and 20% yields, respectively. In contrast, limited conversion was observed when substrates **4** and **5**, equipped with benzoyloxy and ethoxycarbonyloxy groups, were employed.

2.2. Scope

Having determined the optimal conditions, we subsequently explored the reaction scope using various γ -silyl-substituted allyl acetates (Table 2). The reaction with γ -triphenylsilyl-substituted substrate **6** proceeded at 100 °C to provide the corresponding product **7a** in 76% yield (entry 1). Moreover, the reaction tolerated both electron-deficient and electron-rich aryl groups such as those in **8** and **10**. Thus, the reaction of **8** gave migration products **9** in 86% yield (entry 2). When substrate **10** possessing an electron-donating group on the aromatic ring was subjected to the reaction, a longer time was required to achieve full conversion to **11**. This indicates that the formation of silicate intermediates is facilitated when electron-withdrawing substituents are attached to silicon. In addition, no alkene isomerization in products **11a** was observed if

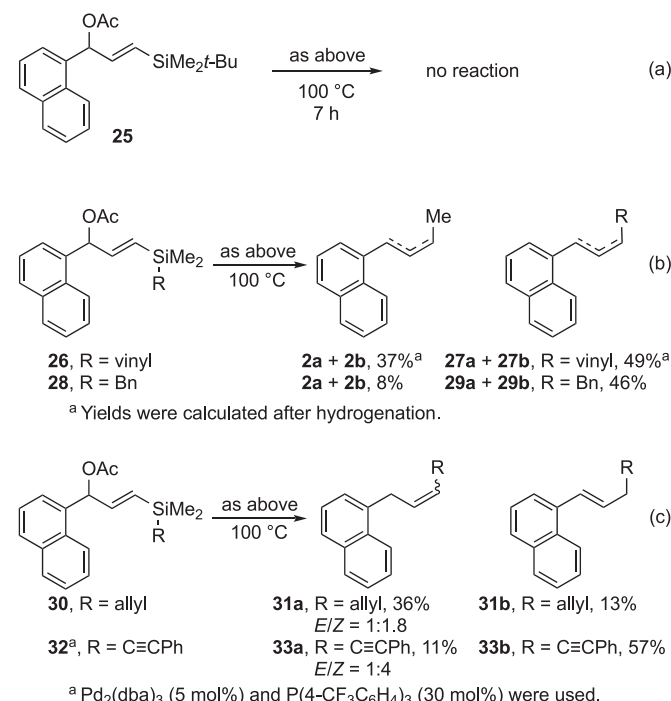


Scheme 4. Relative migratory aptitudes and crossover experiments.

the reaction time was prolonged. Substrates **12** and **14**, bearing heteroaryl substituents (2-furyl and 2-thienyl), were also employed, with both providing high yields (entries 4 and 5). The reaction proceeded with triethylsilyl-substituted substrate **16** (entry 6); the moderate yield of **17** was likely due to its volatility. Interestingly, no β -hydrogen elimination products such as allylbenzene or 1-phenyl-1-propene were observed, which might rule out pathways involving σ -ethylpalladium(II) intermediates. An attempt to use triisopropylsilyl-substituted substrate **18** resulted in no reaction, and **18** was recovered in 78% yield (entry 7).

2.3. Study on relative migratory aptitudes

Next, we evaluated the relative migration aptitude of 1,2-shift of a substituent on silicon. In cases with both methyl and aryl groups, such as γ -dimethylphenylsilyl-substituted allyl acetate **20**, migration from silicon took place with a moderate but not exclusive preference for the phenyl group over the methyl group (Scheme 4a). To obtain further insight into the migration tendency, a 1:1 mixture of **1** and **22** was subjected to the optimal reaction conditions (Scheme 4b). After quenching at an early stage of the reaction (100 °C, 2 h), products **2** and **21** were isolated in 16% and 22% yields, respectively. No crossover products were observed. In addition, this crossover experiment provides additional information about the kinetics of the reaction, clearly revealing that the phenyl group migrated about 1.4 times faster than the methyl group. Even when the crossover experiment was carried out until completion of the reaction, no crossover products were observed (Scheme 4c). As in the case of **16** (Table 2, entry 6), no β -hydride elimination products from **23**, such as 1-(2-propenyl)naphthalene or 1-(1-propenyl)naphthalene, were observed. If the protodesilylation of **1** occurs at the early stage of the reaction, the resulting π -allylpalladium intermediate and silicate species would undergo the intermolecular coupling reaction. To assess such possibility, the palladium-catalyzed reaction of **1** with water was examined in the presence of 1-(3-methoxyphenyl)-2-propenyl acetate (Scheme 4d) [39]. As a



Scheme 5. Approximate orders of migratory aptitude.

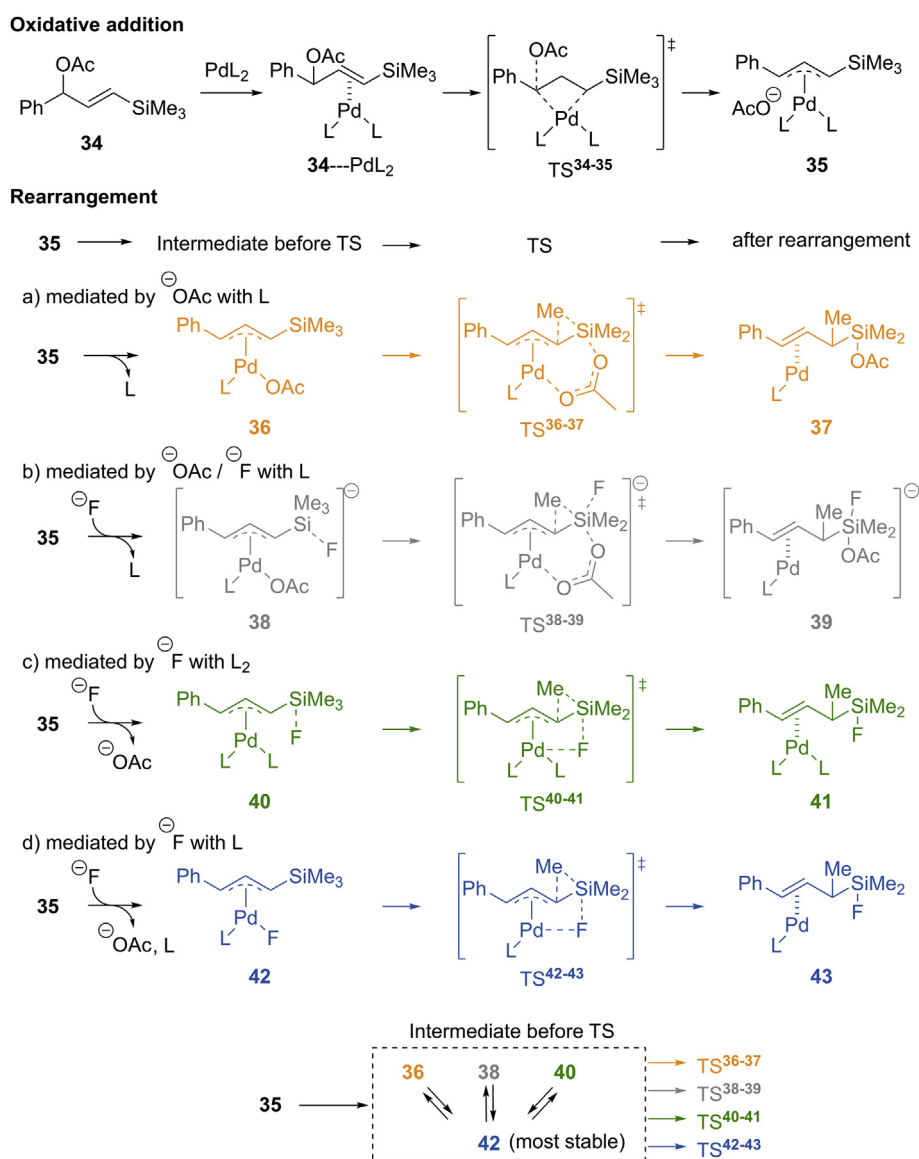
result, **2a** and **2b** were obtained in 61% and 13% yields, respectively and 3-(3-methoxyphenyl)-2-propenyl acetate was recovered in 75%. These results indicate that the migration of a substituent on silicon proceeds in an intramolecular manner.

Subsequently, we explored the approximate relative order of migratory aptitude. Steric hindrance around the silicon atom has a significant influence on the reaction outcome. For example, as in the case of substrate **18**, tert-butyldimethylsilyl-substituted substrate **25** underwent no reaction (Scheme 5a). Changing the tert-butyl group of **25** to a vinyl group afforded methyl migration products **2** and vinyl migration products **27** as a mixture of conjugated diene **27a** and skipped diene **27b**. This result indicated that the vinyl group has a migratory aptitude similar to that of a phenyl group (Scheme 5b). The yields of **2** and **27** were determined after hydrogenation. More selective migration was observed in benzyldimethylsilyl-substituted substrate **28**. Interestingly, the reaction of γ -allyldimethylsilyl-substituted allyl acetate **30** showed an exclusive preference for allyl group migration over that of a methyl group to give **31a** and **31b**, respectively (Scheme 5c). Similarly, we found that a phenylethynyl group had a greater

migratory aptitude than a methyl group, although slightly modified reaction conditions were required to give products in good yields. Nevertheless, the present reaction system provides synthetically useful 1,3-enyne **33a** and skipped enyne **33b** in 11% and 57% yield, respectively. Based on these experiments, the approximate order of migratory aptitude was found to be $\text{PhC}\equiv\text{C}$, allyl > Bn > Ph, vinyl > alkyl (Me, Et); this trend is similar to that observed for the previously reported thermal rearrangements of α -acetoxy silanes [28].

2.4. DFT calculations of the reaction mechanism

Finally, the detailed mechanism of the 1,2-shift reaction was considered (Scheme 6). In the reaction of substrate **34**, oxidative addition of PdL_2 ($\text{L} = \text{P}(4\text{-CF}_3\text{C}_6\text{H}_4)_3$) occurs in the first step to give π -allyl PdL_2 complex **35**, similarly to the Tsuji-Trost reaction. Since the reaction proceeds in an intramolecular manner, as experimentally confirmed above, the subsequent migration of the methyl group should proceed through a transition state in which Si–C bond breaking and C–C bond forming occur simultaneously. The



Scheme 6. Plausible migration models in the presence or absence of fluoride anion.

acceleration effect of the fluoride anion (Table 1, entries 16 and 17) obviously involves activation of the silicon atom in the transition state of migration, considering past reports (see Scheme 1) [26,27]. Therefore, plausible migration models in the presence or absence of fluoride anions were proposed as follows: a) activation with acetate anion (36-TS³⁶⁻³⁷-37), b) activation with acetate and fluoride anions (38-TS³⁸⁻³⁹-39), c) activation with fluoride anion in the presence of L₂ (40-TS⁴⁰⁻⁴¹-41), and d) activation with fluoride anion in the presence of L (42-TS⁴²⁻⁴³-43). The proposed mechanisms were evaluated on the basis of density functional theory (DFT) calculations.

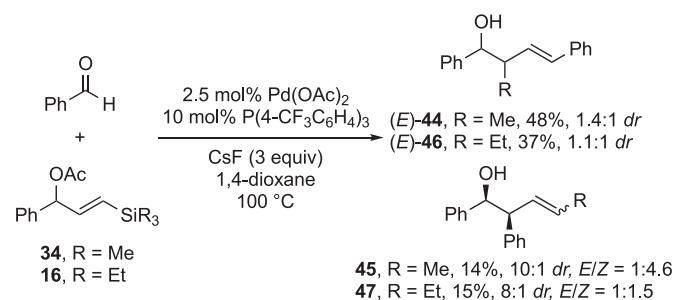
All structures, including transition states, were fully optimized and characterized using frequency calculations at the B3LYP-D3 level with the 6-31+G(d,p) basis set for the organic molecules and the LanL2DZ basis set (with effective core potentials) for palladium and cesium atoms using Gaussian 16, revision C.01 [40]. The structures of the transition states were checked by intrinsic reaction coordinate (IRC) calculations [41]. The Gibbs free energies were initially computed for the gas phase. The relative Gibbs free energies in 1,4-dioxane were obtained using single-point energy calculations of the optimized structures at the B3LYP-D3 functional with the 6-31+G(2d,p) basis set for the organic molecules and the LanL2DZ basis set with the SCRf method based on CPCM followed by the addition of thermal corrections, which were calculated using the above-mentioned geometrical optimizations. The calculation results are shown in Fig. 1.

The ligand exchange of π -allyl Pd complexes (35, 36, 38, 40, 42) should occur easily, and the most stable complex is π -allyl Pd(L)F complex 42 (relative free energy, $\Delta G = -27.0$ kcal/mol), indicating that it is in a resting state. In other words, all equilibrium intermediates (36, 38, 40) drop in at resting state 42 before proceeding to the respective transition state for each pathway. The subsequent migration of the methyl group starts from complex 42 and proceeds through each transition state after ligand exchange. Therefore, the activation energies (ΔG^\ddagger) were calculated by the

differences in energy between 42 and the individual transition states (TS³⁶⁻³⁷, TS³⁸⁻³⁹, TS⁴⁰⁻⁴¹, TS⁴²⁻⁴³). The smallest ΔG^\ddagger (22.8 kcal/mol) for the migration step occurs in pathway d), that is, activation with the fluoride anion in the presence of L, and is a reasonable energy value for the reaction to proceed. In contrast, the ΔG^\ddagger (34.3 kcal/mol) for the migration activated with the acetate anion, pathway a), is too large for the reaction to proceed. These results are identical to the experimental findings (Table 1, entry 7 vs. 16 or 17). In a similar manner, pathways b) and c) are not practical because of their high ΔG^\ddagger values ($\Delta G^\ddagger = 69.6$ and 35.7 kcal/mol, respectively). These theoretical considerations suggest that the migration step proceeds via pathway d). The activation energy of the migration step is higher than that of the oxidative addition (22.8 kcal/mol vs. 21.0 kcal/mol), indicating that the rate-determining step is migration.

2.5. Allylation of aldehydes with in situ-generated α,γ -disubstituted allylsilanes

As the in situ formation of α,γ -disubstituted allylsilanes was supported based on the above experimental results and theoretical



Scheme 7. Allylation of benzaldehyde with 34 and 16.

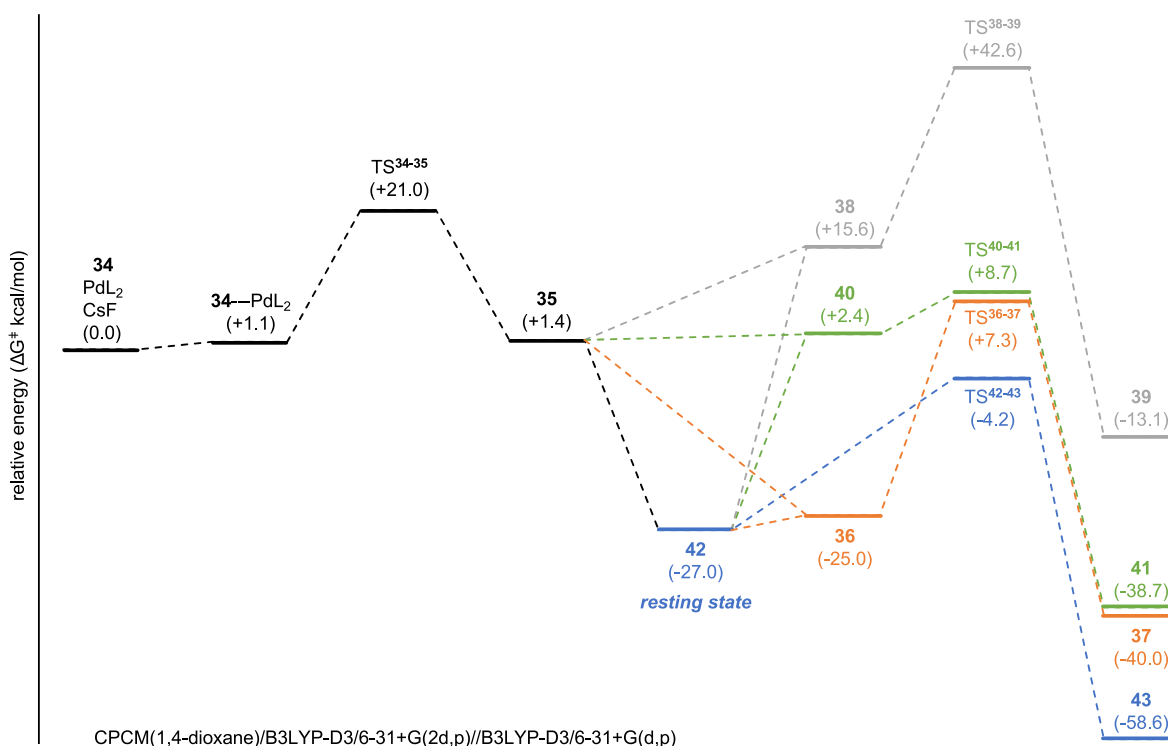
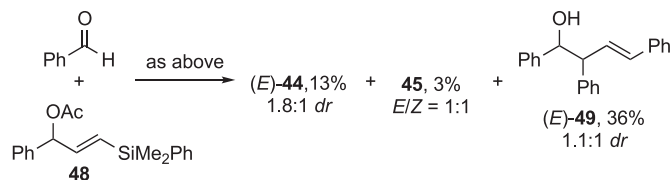


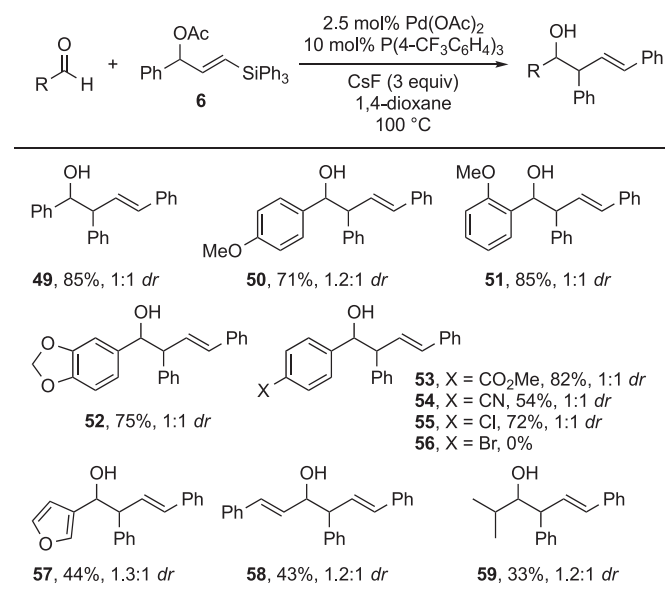
Fig. 1. Computed reaction profiles (CPCM(1,4-dioxane)/B3LYP-D3/6-31+G(2d,p)/LanL2DZ//B3LYP-D3/6-31+G(d,p)/LanL2DZ).

Scheme 8. Alkylation of benzaldehyde with **48**.

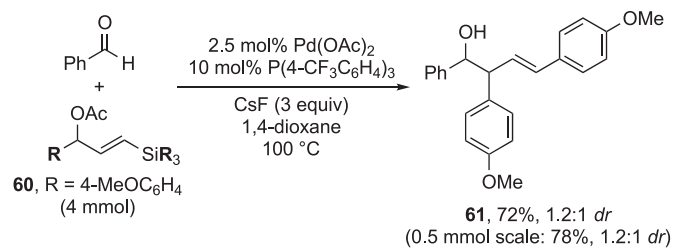
studies, we next assessed their applicability in the Hosomi–Sakurai-type allylation of aldehydes. Using the optimized reaction conditions, the reaction of **34** with benzaldehyde afforded α -adduct (**E**)-**44** in 48% yield as a mixture of diastereomers (syn/anti = 1.4:1), along with γ -adduct **45** in 14% yield as a 1:4.6 mixture of (*E*)-syn and (*Z*)-syn isomers (Scheme 7). Similarly, the allylation of benzaldehyde with **16** gave diastereomeric mixture of (*E*)-**46** and *E/Z* mixture of **47** in 37% and 15% yields, respectively. Due to the intrinsic instability of the hypervalent allylsilane species generated in this system, the current reaction gives homoallylic alcohols as a mixture of regioisomers. According to the pioneering work of Hosomi and Sakurai, fluoride-ion-mediated carbonyl allylation with allylsilanes has also been known to be non-regioselective [42–44].

As in the case of Scheme 4a, the use of **48** possessing a dimethylphenylsilyl group instead of a trimethylsilyl group showed a moderate migration preference for the phenyl group over the methyl group in the allylation of benzaldehyde. As a result, phenyl migration product (*E*)-**49** was obtained in 36% yield as a mixture of diastereomers (1.1:1 *dr*) along with methyl migration products (*E*)-**44** (1.8:1 *dr*) and **45** in 13% and 3% yields, respectively (Scheme 8).

To prevent such regio- and migration-selectivity issues, we chose substrate **6**, which generates α,γ -diphenyl allylsilanes in situ, and investigated the scope of the aldehyde partner (Scheme 9). Reaction with various aromatic aldehydes having different electronic properties proceeded smoothly to afford (*E*)-homoallylic alcohols **49–54** as mixtures of diastereomers. 4-



^a Conditions: **6** (0.5 mmol), aldehyde (1.8 mmol), Pd(OAc)₂ (2.5 mol%), P(4-CF₃C₆H₄)₃ (10 mol%), CsF (1.5 mmol) in 1,4-dioxane (2 mL) at 100 °C.

Scheme 9. Alkylation of aldehydes with in situ-generated α,γ -diphenyl allylsilanes from **6**.

Scheme 10. Gram-scale reaction.

Chlorobenzaldehyde was compatible with this transformation and produced (*E*)-**55** in 72% isolated yield. However, 4-bromobenzaldehyde did not take part in this allylation reaction and starting material was recovered. Furthermore, 3-furancarboxaldehyde could be effectively transformed into desired (*E*)-homoallylic alcohol **57** in 44% isolated yield, and α,β -unsaturated cinnamaldehyde led to the formation of the expected product (*E*)-**58** in 43% yield. Typically, less reactive aliphatic aldehydes were reluctant to undergo this reaction, compared to their aromatic counterparts. Thus, the reaction of isobutyraldehyde gave **59** in 33% yield.

Finally, the scalability of this reaction was demonstrated by a gram-scale experiment using **60**, from which **61** was obtained in 72% yield (Scheme 10).

3. Conclusion

We have developed a palladium-catalyzed reaction of readily accessible γ -silylated allyl acetates with water in the presence of CsF, which induces a previously unprecedented 1,2-shift of a substituent on silicon in the silylated π -allylpalladium intermediates. The key to the success of this reaction is the use of an electron-poor phosphine ligand possessing fluorinated substituents. Theoretical studies indicate that the 1,2-shift of the substituent on the silicon atom proceeds through a transition state assisted by the fluoride anion, where the migration step is rate-determining. In addition, the Hosomi–Sakurai-type allylation of aldehydes with in situ-generated α,γ -disubstituted allylsilanes successfully provided homoallylic alcohols with good functional group compatibility. Further investigations to elucidate the reaction mechanism, including the stereoselectivity of this process, and to develop regio- and diastereoselective carbonyl allylations, including in an intramolecular fashion, are now ongoing in our laboratory.

4. Experimental section

4.1. General experimental information

All reactions were carried out in flame-dried glassware under an argon atmosphere. Tetrahydrofuran (THF) and 1,4-dioxane were dried over Na with benzophenone-ketyl intermediate as indicator. Triethylamine, diisopropylamine, and dichloromethane were purified by distillation from CaH₂. All commercial reagents were used as received unless otherwise noted. Flash chromatography was performed with Fuji Silysia PSQ100B (100 μ m). Thin layer chromatography (TLC) was carried out using Silicagel 70 F254 TLC Plate-Wako. NMR spectra were recorded on JEOL α -GX400 or JNX-ECX500 spectrometer. For ¹H NMR, tetramethylsilane (TMS) served as internal standard (δ = 0 ppm) and data are reported as follows: chemical shift, integration, multiplicity (*s* = singlet; *d* = doublet; *t* = triplet; *q* = quartet; *m* = multiplet; *br* = broad), and coupling constant(s) in (J) Hz. For ¹³C NMR, CDCl₃

($\delta = 77.16$ ppm) was used as internal standard and spectra were obtained with complete proton decoupling. High-resolution mass (HRMS) spectral data were obtained on a JEOL MStation JMS-700.

4.2. General procedure for the synthesis of **2a** and **2b** (Table 1, entry 7)

A 10 mL two neck round-bottom flask was charged with Pd(OAc)₂ (5.6 mg, 0.025 mmol), P(4-CF₃C₆H₄)₃ (46.7 mg, 0.1 mmol), and 1,4-dioxane (1.5 mL) under an argon atmosphere. The mixture was stirred at 80 °C for 0.5 h and cooled to room temperature, which was then transferred into another 10 mL two neck round-bottom flask charged with cesium fluoride (227.8 mg, 1.5 mmol). To this mixture was subsequently added **1** (149.2 mg, 0.5 mmol) and H₂O (10.8 mg, 0.6 mmol) in 1,4-dioxane (1.5 mL) via cannula. The reaction mixture was stirred at 100 °C for 6 h. Upon completion of the reaction, the mixture was filtered through a pad of Celite with diethyl ether (20 mL) as the washing solvent. The filtrate was washed with saturated NH₄Cl (2 × 20 mL) and brine (2 × 20 mL). The combined organic layers were dried over MgSO₄ and concentrated. The residue was purified by silica gel column chromatography (R_f 0.66: EtOAc/hexane = 1:4) to give **2a** (56.1 mg, 62%, E/Z = 1:7.2) and **2b** (13.1 mg, 14%) as an inseparable mixture (colorless oil).

4.3. Characterization data of newly synthesized compounds

4.3.1. (Z)-1-(But-2-en-1-yl)naphthalene (**2a**) [45]

The ¹H NMR spectrum of (Z)-**2a** was identical with that reported in the literature [45]. ¹H NMR (CDCl₃, 400 MHz) δ 8.08 (m, 1H), 7.90–7.88 (m, 1H), 7.77 (m, 1H), 7.61–7.36 (m, 4H), 5.81–5.55 (m, 2H), 3.88 (d, J = 5.2 Hz, 2H), 1.85 (d, J = 5.6 Hz, 3H).

4.3.2. (E)-1-(But-2-en-1-yl)naphthalene (**2a**) [46]

The ¹H NMR spectrum of (E)-**2a** was identical with that reported in the literature [46]. ¹H NMR (CDCl₃, 400 MHz) δ 8.08 (m, 1H), 7.88 (m, 1H), 7.77 (m, 1H), 7.61–7.36 (m, 4H), 5.81–5.55 (m, 2H), 3.81 (d, J = 6.0 Hz, 2H), 1.72 (dd, J = 1.2, 6.8 Hz, 3H).

4.3.3. (E)-1-(But-1-en-1-yl)naphthalene (**2b**) [47]

The ¹H NMR spectrum of (E)-**2b** was identical with that reported in the literature [47]. ¹H NMR (CDCl₃, 400 MHz) δ 8.18 (d, J = 8.0 Hz, 1H), 7.90–7.36 (m, 6H), 7.16 (d, J = 16.0 Hz, 1H), 6.32 (dt, J = 16.0, 6.4 Hz, 1H), 2.43–2.35 (m, 2H), 1.22 (t, J = 7.6 Hz, 3H).

4.3.4. (E)-1-(3-(trimethylsilyl)prop-1-en-1-yl)naphthalene (**2c**) [48]

The ¹H NMR spectrum of (E)-**2c** was identical with that reported in the literature [48]. ¹H NMR (CDCl₃, 400 MHz) δ 8.13 (dm, J = 8.0 Hz, 1H), 7.83 (dm, J = 8.0 Hz, 1H), 7.72 (dm, J = 8.0 Hz, 1H), 7.53–7.40, 6.96 (d, J = 16.0 Hz, 1H), 6.26 (dt, J = 16.0, 8.0 Hz, 1H), 1.81 (dd, J = 1.2, 8.0 Hz, 1H), 0.11 (2, 9H).

4.3.5. (Z)-1,3-Diphenylpropene (**7a**) [49]

(Z)-**7a** and (E)-**7a** were isolated as an inseparable mixture (0.5 mmol scale reaction, 73.7 mg, 76%, E/Z = 17.5:1, colorless oil, R_f 0.23: hexane). The ¹H NMR spectrum of (Z)-**7a** was identical with that reported in the literature [49]. ¹H NMR (CDCl₃, 400 MHz) δ 7.39–7.20 (m, 10H), 6.61 (d, J = 11.6 Hz, 1H), 5.88 (dt, J = 11.6, 8.0 Hz, 1H), 3.70 (d, J = 8.0 Hz, 2H).

4.3.6. (E)-1,3-Diphenylpropene (**7a**) [49]

The ¹H NMR spectrum of (E)-**7a** was identical with that reported in the literature [49]. ¹H NMR (CDCl₃, 400 MHz) δ 7.39–7.20 (m, 10H), 6.48 (d, J = 16.0 Hz, 1H), 6.38 (dt, J = 16.0, 6.8 Hz, 1H), 3.57 (d,

J = 6.8 Hz, 2H).

4.3.7. (E)-1-(3-Phenylprop-1-en-1-yl)-4-(trifluoromethyl)benzene (**9a**) [50]

(E)-**9a** and (E)-**9b** were isolated as an inseparable mixture (0.5 mmol scale reaction, 113.2 mg, 86%, **9a/9b** = 1:2.1, colorless oil, R_f 0.59: EtOAc/hexane = 1:4). The ¹H NMR spectrum of (E)-**9a** was identical with that reported in the literature [50]. ¹H NMR (CDCl₃, 400 MHz) δ 7.53 (d, J = 8.4 Hz, 2H), 7.43 (d, J = 8.4 Hz, 2H), 7.37–7.20 (m, 5H), 6.49–6.45 (m, 2H), 3.57 (d, J = 3.6 Hz, 2H).

4.3.8. (E)-1-Cinnamyl-4-(trifluoromethyl)benzene (**9b**) [50]

The ¹H NMR spectrum of (E)-**9b** was identical with that reported in the literature [50]. ¹H NMR (CDCl₃, 400 MHz) δ 7.56 (d, J = 8.0 Hz, 2H), 7.37–7.20 (m, 7H), 6.47 (m, 1H), 6.32 (dt, J = 16.0, 6.8 Hz, 1H), 3.60 (d, J = 6.8 Hz, 2H).

4.3.9. (Z)-1-Methoxy-4-(3-phenylprop-1-en-1-yl)benzene (**11a**) [51]

(Z)-**11a**, (E)-**11a**, and **11b** were isolated as an inseparable mixture (1 mmol scale reaction, 177.3 mg, 84%, (Z)-**11a**/(E)-**11a/11b** = 1:3.2:2.7, colorless oil, R_f 0.54: EtOAc/hexane = 1:4). The ¹H NMR spectrum of (Z)-**11a** was identical with that reported in the literature [51]. ¹H NMR (CDCl₃, 400 MHz) δ 7.36–7.14 (m, 7H), 6.89 (m, 2H), 6.53 (d, J = 11.6 Hz, 1H), 5.77 (dt, J = 11.6, 7.2 Hz, 1H), 3.81 (s, 3H), 3.67 (dd, J = 1.6, 7.2 Hz, 2H).

4.3.10. (E)-1-Methoxy-4-(3-phenylprop-1-en-1-yl)benzene (**11a**) [51]

The ¹H NMR spectrum of (E)-**11a** was identical with that reported in the literature [51]. ¹H NMR (CDCl₃, 400 MHz) δ 7.36–7.14 (m, 7H), 6.89 (m, 2H), 6.45–6.38 (m, 1H), 6.21 (dt, J = 16.0, 7.2 Hz, 1H), 3.79 (s, 3H), 3.53 (d, J = 6.8 Hz, 2H).

4.3.11. (E)-1-Cinnamyl-4-methoxybenzene (**11b**) [52]

The ¹H NMR spectrum of (E)-**11b** was identical with that reported in the literature [52]. ¹H NMR (CDCl₃, 400 MHz) δ 7.36–7.14 (m, 7H), 6.89 (m, 2H), 6.45–6.38 (m, 1H), 6.33 (dt, J = 15.6, 6.4 Hz, 1H), 3.79 (s, 3H), 3.49 (d, J = 6.4 Hz, 2H).

4.3.12. (Z)-2-(3-Phenylprop-1-en-1-yl)furan (**13a**) [50]

(Z)-**13a**, (E)-**13a**, and **13b** were isolated as an inseparable mixture (0.5 mmol scale reaction, 57.3 mg, 64%, (Z)-**13a**/(E)-**13a/13b** = 1:1:3.2, colorless oil, R_f 0.59: EtOAc/hexane = 1:4). The ¹H NMR spectrum of (Z)-**13a** was identical with that reported in the literature [50]. ¹H NMR (CDCl₃, 400 MHz) δ 7.41–7.19 (m, 6H), 6.42–6.25 (m, 3H), 5.71 (dt, J = 11.6, 7.6 Hz, 1H), 3.84 (dd, J = 0.8, 7.6 Hz, 2H).

4.3.13. (E)-2-(3-Phenylprop-1-en-1-yl)furan (**13a**) [50]

The ¹H NMR spectrum of (E)-**13a** was identical with that reported in the literature [50]. ¹H NMR (CDCl₃, 400 MHz) δ 7.41–7.19 (m, 6H), 6.42–6.25 (m, 3H), 6.15 (d, J = 3.2 Hz, 1H), 3.51 (d, J = 6.8 Hz, 2H).

4.3.14. (E)-2-Cinnamylfuran (**13b**) [52]

The ¹H NMR spectrum of (E)-**13b** was identical with that reported in the literature [52]. ¹H NMR (CDCl₃, 400 MHz) δ 7.41–7.19 (m, 6H), 6.49 (d, J = 15.6 Hz, 1H), 6.42–6.25 (m, 2H), 6.07 (dd, J = 0.8, 3.2 Hz, 1H), 3.55 (d, J = 6.8 Hz, 2H).

4.3.15. (Z)-2-(3-Phenylprop-1-en-1-yl)thiophene (**15a**) [53]

(Z)-**15a**, (E)-**15a**, and **15b** were isolated as an inseparable mixture (0.5 mmol scale reaction, 61.5 mg, 62%, (Z)-**15a**/(E)-**15a/15b** = 1:1.2:8.3, yellow solid, R_f 0.68: EtOAc/hexane = 1:4). The ¹H

NMR spectrum of (Z)-**15a** was identical with that reported in the literature [53]. ^1H NMR (CDCl_3 , 400 MHz) δ 7.39–7.20 (m, 5H), 7.03 (m, 1H), 6.97–6.87 (m, 2H), 6.66 (d, $J = 10.8$ Hz, 1H), 5.80–5.73 (m, 1H), 3.79 (d, $J = 7.2$ Hz, 2H).

4.3.16. (E)-2-(3-Phenylprop-1-en-1-yl)thiophene (**15a**) [53]

The ^1H NMR spectrum of (E)-**15a** was identical with that reported in the literature [53]. ^1H NMR (CDCl_3 , 400 MHz) δ 7.39–7.20 (m, 5H), 7.05–7.00 (m, 1H), 6.97–6.87 (m, 2H), 6.55 (d, $J = 16.8$ Hz, 1H), 6.23 (m, 1H), 3.51 (d, $J = 6.8$ Hz, 2H).

4.3.17. (E)-2-Cinnamylthiophene (**15b**) [52]

The ^1H NMR spectrum of (E)-**15b** was identical with that reported in the literature [52]. ^1H NMR (CDCl_3 , 400 MHz) δ 7.39–7.20 (m, 5H), 7.17–7.16 (m, 1H), 6.95 (m, 1H), 6.88 (m, 1H), 6.51 (d, $J = 16.0$ Hz, 1H), 6.37 (m, 1H), 3.74 (d, $J = 6.4$ Hz, 2H).

4.3.18. (Z)-Pent-2-en-1-ylbenzene (**17a**) [54]

(Z)-**17a**, (E)-**17a**, and **17b** were isolated as an inseparable mixture (0.5 mmol scale, reaction, 34.8 mg, 48%, (Z)-**17a**/(E)-**17a**/**17b** = 3.3:1:2, colorless oil, R_f 0.72: EtOAc/hexane = 1:4). The ^1H NMR spectrum of (Z)-**17a** was identical with that reported in the literature [54]. ^1H NMR (CDCl_3 , 400 MHz) δ 7.36–7.19 (m, 5H), 5.58–5.51 (m, 2H), 3.41 (d, $J = 6.0$ Hz, 2H), 2.22–2.02 (m, 2H), 1.05–0.94 (m, 3H).

4.3.19. (E)-Pent-2-en-1-ylbenzene (**17a**) [55]

The ^1H NMR spectrum of (E)-**17a** was identical with that reported in the literature [55]. ^1H NMR (CDCl_3 , 400 MHz) δ 7.36–7.19 (m, 5H), 5.58–5.51 (m, 2H), 3.33 (d, $J = 3.6$ Hz, 2H), 2.22–2.02 (m, 2H), 1.05–0.94 (m, 3H).

4.3.20. (E)-Pent-1-en-1-ylbenzene (**17b**) [56]

The ^1H NMR spectrum of (E)-**17b** was identical with that reported in the literature [56]. ^1H NMR (CDCl_3 , 400 MHz) δ 7.36–7.19 (m, 5H), 6.39 (d, $J = 15.6$ Hz, 1H), 6.23 (dt, $J = 15.6, 6.8$ Hz, 1H), 2.22–2.02 (m, 2H), 1.55–1.46 (m, 2H), 1.05–0.94 (m, 3H).

4.3.21. (Z)-1-(3-Phenylallyl)naphthalene (**21a**)

(Z)-**21a**, (E)-**21a**, and **21b** were isolated as an inseparable mixture (1 mmol scale reaction, 82.6 mg, 35%, (Z)-**21a**/(E)-**21a**/**21b** = 1:9.2:6.1, yellow solid, R_f 0.57: EtOAc/hexane = 1:4); Yellow solid; ^1H NMR (CDCl_3 , 400 MHz) δ 8.08 (m, 1H), 7.85–7.13 (m, 11H), 6.61 (d, $J = 11.6$ Hz, 1H), 5.91 (dt, $J = 11.6, 7.2$ Hz, 1H), 4.08 (d, $J = 7.2$ Hz, 2H); ^{13}C NMR (CDCl_3 , 100 MHz) δ 137.4, 136.9, 135.1, 134.8, 134.5, 130.9, 130.7, 130.3, 128.2, 128.0, 127.8, 127.0, 32.4; HRMS (EI): found 244.1251. $\text{C}_{19}\text{H}_{16}$ requires 244.1252.

4.3.22. (E)-1-(3-Phenylallyl)naphthalene (**21a**) [57]

The ^1H NMR spectrum of (E)-**21a** was identical with that reported in the literature [57]. ^1H NMR (CDCl_3 , 400 MHz) δ 8.08 (m, 1H), 7.85–7.13 (m, 11H), 6.49 (dd, $J = 5.6, 16.0$ Hz, 1H), 6.43 (d, $J = 16.0$ Hz, 1H), 3.96 (d, $J = 4.4$ Hz, 2H).

4.3.23. (E)-1-(3-Phenylprop-1-en-1-yl)naphthalene (**21b**) [58]

The ^1H NMR spectrum of (E)-**21b** was identical with that reported in the literature [58]. ^1H NMR (CDCl_3 , 400 MHz) δ 8.08 (m, 1H), 7.85–7.13 (m, 12H), 6.36 (dt, $J = 15.2, 6.8$ Hz, 1H), 3.64 (d, $J = 6.8$ Hz, 2H).

4.3.24. (Z)-1-(Pent-2-en-1-yl)naphthalene (**24a**)

(Z)-**24a**, (E)-**24a**, and **24b** were isolated as an inseparable mixture (0.5 mmol scale reaction, 81.0 mg, 82%, (Z)-**24a**/(E)-**24a**/**24b** = 2.1:1:1, colorless oil, R_f 0.72: EtOAc/hexane = 1:4). ^1H NMR (CDCl_3 , 400 MHz) δ 8.06–8.01 (m, 1H), 7.84 (m, 1H), 7.72 (m, 1H),

7.56–7.32 (m, 5H), 5.64–5.52 (m, 2H), 3.83 (d, $J = 6.4$ Hz, 2H), 2.25 (quint, $J = 7.2$ Hz, 2H), 1.06 (t, $J = 7.2$ Hz, 3H); For (Z)-**24a** and (E)-**24a**: ^{13}C NMR (CDCl_3 , 100 MHz) δ 137.4, 137.3, 134.02 (two peaks), 133.98, 133.95, 132.9 (two peaks), 132.1, 128.83, 128.76, 127.4, 127.3, 126.9, 126.8, 126.1, 125.9 (two peaks), 125.8 (two peaks), 125.6, 124.2, 124.0, 36.2, 31.0, 25.7, 20.9, 14.4, 13.9; HRMS (EI): found 196.1252. $\text{C}_{15}\text{H}_{16}$ requires 196.1252.

4.3.25. (E)-1-(Pent-2-en-1-yl)naphthalene (**24a**)

^1H NMR (CDCl_3 , 400 MHz) δ 8.04 (m, 1H), 7.84 (m, 1H), 7.72 (m, 1H), 7.56–7.32 (m, 5H), 5.73–5.66 (m, 2H), 3.77 (d, $J = 6.4$ Hz, 2H), 2.03 (dq, $J = 1.2, 7.2$ Hz, 2H), 0.97 (t, $J = 7.2$ Hz, 3H).

4.3.26. (E)-1-(Pent-1-en-1-yl)naphthalene (**24b**) [59]

The ^1H NMR spectrum of (E)-**24b** was identical with that reported in the literature [59]. ^1H NMR (CDCl_3 , 400 MHz) δ 8.12 (d, $J = 7.2$ Hz, 1H), 7.84 (m, 1H), 7.72 (m, 1H), 7.55 (d, $J = 7.6$ Hz, 1H), 7.53–7.32 (m, 3H), 7.11 (d, $J = 15.2$ Hz, 1H), 6.23 (dt, $J = 15.2, 7.2$ Hz, 1H), 2.34–2.30 (m, 2H), 1.57 (sext, $J = 7.2$ Hz, 2H), 1.01 (t, $J = 7.2$ Hz, 3H).

4.3.27. 1-Butylnaphthalene [60]

2a, **2b**, (Z)-1-(penta-2,4-dien-1-yl)naphthalene (**27a**), and (E)-1-(penta-1,4-dien-1-yl)naphthalene (**27b**) were isolated as an inseparable mixture. The hydrogenation of given alkenes was performed to identify the products. To a solution of **2** and **27** (160.0 mg) in ethyl acetate (3 mL) was added Pd/C (106.4 mg). The atmosphere in the flask was replaced to hydrogen under balloon pressure, and the mixture was vigorously stirred at room temperature for 12 h. Upon completion, the mixture was filtered through a pad of Celite to afford crude material, which was purified by silica gel column chromatography to give 1-butylnaphthalene (37%) and 1-pentylnaphthalene (49%) as an inseparable mixture (165.1 mg, R_f 0.65: EtOAc/hexane = 1:4, colorless oil).

1-Butylnaphthalene [60]: The ^1H NMR spectrum of 1-butylnaphthalene was identical with that reported in the literature [57]. ^1H NMR (CDCl_3 , 400 MHz) δ 8.03 (d, $J = 7.6$ Hz, 1H), 7.82 (d, $J = 8.0$ Hz, 1H), 7.68 (d, $J = 8.0$ Hz, 1H), 7.50–7.42 (m, 2H), 7.36 (d, $J = 7.6$ Hz, 1H), 7.29 (d, $J = 6.8$ Hz, 1H), 3.05 (t, $J = 7.6$ Hz, 2H), 1.78–1.68 (m, 2H), 1.49–1.33 (m, 2H), 0.96 (t, $J = 7.6$ Hz, 3H).

4.3.28. 1-Pentylnaphthalene [61]

The ^1H NMR spectrum of 1-pentylnaphthalene was identical with that reported in the literature [58]. ^1H NMR (CDCl_3 , 400 MHz) δ 8.03 (d, $J = 7.6$ Hz, 1H), 7.82 (d, $J = 8.0$ Hz, 1H), 7.68 (d, $J = 8.0$ Hz, 1H), 7.50–7.42 (m, 2H), 7.37 (t, $J = 7.6$ Hz, 1H), 7.29 (d, $J = 6.8$ Hz, 1H), 3.04 (t, $J = 7.6$ Hz, 2H), 1.78–1.68 (m, 2H), 1.49–1.33 (m, 4H), 0.90 (t, $J = 6.8$ Hz, 3H).

4.3.29. (E)-1-(4-Phenyl-2-buten-1-yl)naphthalene (**29a**)

(Z)-**29a**, (E)-**29a**, and **29b** were isolated as an inseparable mixture (0.5 mmol scale reaction, 58.4 mg, 46%, (Z)-**29a**/(E)-**29a**/**29b** = 2.6:1.3:1, colorless oil, R_f 0.60: EtOAc/hexane = 1:4). The alkene stereochemistry was determined by the analysis of nOe experiments. For details, see the supplementary material.

(Z)-isomer: ^1H NMR (CDCl_3 , 400 MHz) δ 8.03 (m, 1H), 7.84 (m, 1H), 7.74 (m, 1H), 7.52–7.15 (m, 9H), 5.84–5.66 (m, 2H), 3.95 (d, $J = 5.6$ Hz, 2H), 3.61 (d, $J = 6.0$ Hz, 2H); For (E)- and (Z)-isomers, ^{13}C NMR (CDCl_3 , 100 MHz) δ 140.84, 140.80, 136.93, 136.89, 134.00, 133.97, 132.1, 131.3, 130.8, 129.5, 129.0, 128.88, 128.80, 128.64, 128.58, 128.48, 127.0, 126.2, 126.14, 126.08, 125.99, 125.7, 125.6, 124.3, 124.0, 39.1, 36.3, 33.8, 31.1.

Characteristic peaks of (E)-isomer: ^1H NMR (CDCl_3 , 400 MHz)

δ 3.82 (d, $J = 6.4$ Hz, 2H), 3.36 (d, $J = 6.4$ Hz, 2H).

4.3.30. (E)-1-(4-Phenyl-1-buten-1-yl)naphthalene (**29b**) [62]

The ^1H NMR spectrum of (E)-**29b** was identical with that reported in the literature [62]. ^1H NMR (CDCl_3 , 400 MHz) δ 8.03 (m, 1H), 7.84 (m, 1H), 7.72 (d, $J = 8.4$ Hz, 1H), 7.52–7.15 (m, 9H), 7.09 (d, $J = 15.6$ Hz, 1H), 6.24 (dt, $J = 15.6$, 6.8 Hz, 1H), 2.87 (t, $J = 8.0$ Hz, 2H), 2.65 (dq, $J = 0.8$, 7.2 Hz, 2H); ^{13}C NMR (CDCl_3 , 100 MHz) δ 141.8, 135.7, 133.7, 133.3, 130.2, 128.7, 128.52, 128.0, 127.5, 126.04, 125.91, 125.8, 124.1, 123.7, 36.0, 35.3.

4.3.31. 1-(Hexa-2,5-dien-1-yl)naphthalene (**31a**)

(Z)-**31a**, (E)-**31a**, and **31b** were isolated as an inseparable mixture (1 mmol scale reaction, 105.0 mg, 49%, (Z)-**31a**/(E)-**31a**/**31b** = 1.8:1:1, yellow oil, R_f 0.66: EtOAc/hexane = 1:4). The alkene stereochemistry was determined by the analysis of nOe experiments. For details, see the supplementary material.

For (E)- and (Z)-isomers: ^{13}C NMR (CDCl_3 , 100 MHz) δ 137.2, 137.0, 136.9, 136.7, 133.98, 133.95, 132.1, 131.3, 129.8, 129.6, 129.2, 128.84, 128.78, 128.0, 126.9, 126.2, 125.94, 125.87, 124.2, 124.0, 36.8, 36.2, 31.9, 31.0.

4.3.32. (E)-1-(Hexa-1,5-dien-1-yl)naphthalene (**31b**) [63]

The ^1H NMR spectrum of (E)-**31b** was identical with that reported in the literature [63]. ^1H NMR (CDCl_3 , 400 MHz) δ 8.12 (d, $J = 8.0$ Hz, 1H), 7.84 (m, 1H), 7.72 (d, $J = 8.0$ Hz, 1H), 7.55–7.44 (m, 3H), 7.13 (d, $J = 15.6$ Hz, 1H), 6.24 (dt, $J = 6.8$, 16.0 Hz, 1H), 5.83 (m, 1H), 5.05–5.02 (m, 3H), 2.47–2.41 (m, 2H), 2.35–2.29 (m, 2H); ^{13}C NMR (CDCl_3 , 100 MHz) δ 138.2, 135.7, 133.7, 133.5, 128.6, 127.6, 127.4, 125.8, 125.7, 125.6, 124.1, 123.7, 115.2, 33.7, 32.9.

4.3.33. 1-(5-Phenylpent-2-en-4-yn-1-yl)naphthalene (**33a**) [64]

(Z)-**33a**, (E)-**33a**, and **33b** were isolated as an inseparable mixture (0.4 mmol scale reaction, 69.0 mg, 68%, (Z)-**33a**/(E)-**33a**/**33b** = 4:1:26, yellow oil, R_f 0.60: EtOAc/hexane = 1:4). The ^1H NMR spectrum of (Z)-**33a** was identical with that reported in the literature [64]. Characteristic peaks of (Z)-isomer: ^1H NMR (CDCl_3 , 500 MHz) δ 6.17 (t, $J = 7.0$, 10.5 Hz, 1H), 5.83 (dt, $J = 10.5$, 1.5 Hz, 1H), 4.15 (dd, $J = 1.5$, 7.0 Hz, 2H).

Characteristic peaks of (E)-isomer: ^1H NMR (CDCl_3 , 500 MHz) δ 6.54 (t, $J = 6.5$, 16.0 Hz, 1H), 5.72 (dt, $J = 16.0$, 1.5 Hz, 1H), 3.94 (dd, $J = 1.5$, 6.5 Hz, 2H).

4.3.34. (E)-1-(5-phenylpent-1-en-4-yn-1-yl)naphthalene (**33b**)

^1H NMR (CDCl_3 , 500 MHz) δ 8.14 (d, $J = 8.5$ Hz, 1H), 7.85 (dm, $J = 8.5$ Hz, 1H), 7.77 (d, $J = 8.5$ Hz, 1H), 7.58 (d, $J = 7.5$ Hz, 1H), 7.52–7.41 (m, 6H), 7.34–7.28 (m, 3H), 6.26 (dt, $J = 5.5$, 15.0 Hz, 1H), 3.47 (dd, $J = 2.0$, 5.5 Hz, 2H); ^{13}C NMR (CDCl_3 , 100 MHz) δ 135.1, 133.7, 131.8, 131.3, 128.9, 128.6, 128.4, 128.0, 127.9, 127.5, 126.1, 125.9, 125.8, 124.05, 124.02, 123.8, 86.9, 83.3, 23.6; HRMS (EI): found 268.1250. $\text{C}_{21}\text{H}_{16}$ requires 268.1252.

4.4. General procedure for allylation of aldehydes with in situ generated α,γ -disubstituted allylsilanes

A 10 mL two neck round-bottom flask was charged with Pd(OAc)₂ (2.8 mg, 0.0125 mmol), P(4-CF₃C₆H₄)₃ (23.3 mg, 0.05 mmol), and 1,4-dioxane (1.0 mL) under an argon atmosphere. The mixture was stirred at 80 °C for 0.5 h and cooled to room temperature, which was then transferred into another 10 mL two neck round-bottom flask charged with cesium fluoride (227.8 mg, 1.5 mmol). To this mixture was subsequently added **6** (217.3 mg, 0.5 mmol) and benzaldehyde (191.0 mg, 1.8 mmol) in 1,4-dioxane

(1.0 mL) via cannula. The reaction mixture was stirred at 100 °C for 2.5 h. Upon completion of the reaction, the mixture was filtered through a pad of Celite with diethyl ether (20 mL) as the washing solvent. The filtrate was washed with saturated NH₄Cl (2 × 20 mL) and brine (2 × 20 mL). The combined organic layers were dried over MgSO₄ and concentrated. The residue was purified by silica gel column chromatography (R_f 0.33: EtOAc/hexane = 1:4) to give **49** (127.7 mg, 85%, syn/anti = 52:48) as an inseparable mixture (yellow oil).

4.5. Characterization data of newly synthesized compounds

4.5.1. (E)-1,2,4-Triphenylbut-3-en-1-ol (**49**)

syn-**49** and anti-**49** were isolated as an inseparable mixture (116.8 mg, 85%, colorless solid, R_f 0.46: EtOAc/hexane = 3:7). The ^1H NMR spectrum of anti-**49** was identical with that reported in the literature [65]. anti-isomer: ^1H NMR (CDCl_3 , 400 MHz) δ 7.41–7.14 (m, 15H), 6.63 (dd, $J = 7.9$, 15.8 Hz, 1H), 6.53 (d, $J = 15.8$ Hz, 1H), 4.94 (dd, $J = 2.4$, 7.9 Hz, 1H), 3.73 (t, $J = 7.9$ Hz, 1H), 2.37 (d, $J = 2.4$ Hz, 1H); ^{13}C NMR (CDCl_3 , 100 MHz) δ 142.0, 140.9, 137.0, 133.5, 129.2, 128.9, 128.6, 128.52, 128.0, 127.6, 127.5, 126.8, 126.4, 77.8, 58.4.

syn-isomer: ^1H NMR (CDCl_3 , 400 MHz) δ 7.41–7.14 (m, 15H), 6.29 (dd, $J = 7.9$, 15.8 Hz, 1H), 6.18 (d, $J = 15.8$ Hz, 1H), 5.00 (dd, $J = 3.0$, 7.9 Hz, 1H), 3.78 (t, $J = 7.9$ Hz, 1H), 2.05 (d, $J = 3.0$ Hz, 1H); ^{13}C NMR (CDCl_3 , 100 MHz) δ 142.0, 140.5, 137.3, 132.3, 129.5, 128.9, 128.55, 128.3, 127.9, 127.3, 127.2, 127.0, 126.2, 77.9, 57.8.

4.5.2. (E)-2-Methyl-1,4-diphenylbut-3-en-1-ol (**44**) [44]

44 and **45** were isolated as an inseparable mixture (74.7 mg, 60%, yellow oil, R_f 0.40 and 0.38: EtOAc/hexane = 1:4).

The ^1H NMR spectrum of syn-(E)-**44** was identical with that reported in the literature [44].

syn-(E)-**44**: ^1H NMR (CDCl_3 , 400 MHz) δ 7.37–7.17 (m, 10H), 6.42 (d, $J = 16.0$ Hz, 1H), 6.16 (dd, $J = 8.0$, 15.6 Hz, 1H), 4.70 (d, $J = 5.2$ Hz, 1H), 2.77 (sext, $J = 6.8$ Hz, 1H), 2.16 (br s, 1H), 1.14 (d, $J = 6.8$ Hz, 3H).

The ^1H NMR spectrum of anti-(E)-**44** was identical with that reported in the literature [44].

Characteristic peaks of anti-(E)-**44**: ^1H NMR (CDCl_3 , 400 MHz) δ 6.56 (d, $J = 16.0$ Hz, 1H), 6.23 (dd, $J = 16.1$, 8.4 Hz, 1H), 4.47 (d, $J = 8.0$ Hz, 1H), 2.69 (sext, $J = 7.2$ Hz, 1H), 2.23 (br s, 1H), 1.00 (d, $J = 7.2$ Hz, 3H).

4.5.3. (Z)-1,2-Diphenylpent-3-en-1-ol (**45**) [44]

The ^1H NMR spectrum of syn-(Z)-**45** was identical with that reported in the literature [44].

Characteristic peaks of syn-(Z)-**45**: ^1H NMR (CDCl_3 , 400 MHz) δ 5.65 (tq, $J = 10.8$, 1.6 Hz, 1H), 5.45 (dq, $J = 10.8$, 6.8, 0.8 Hz, 1H), 4.85 (d, $J = 8.4$ Hz, 1H), 3.95 (t, $J = 9.2$ Hz, 1H), 2.07 (br s, 1H), 1.36 (dd, $J = 6.8$, 2.0 Hz, 1H).

Characteristic peaks of minor isomer of **45**: ^1H NMR (CDCl_3 , 400 MHz) δ 5.60 (ddq, $J = 15.2$, 8.0, 1.6 Hz, 1H), 5.31 (dq, $J = 15.2$, 6.8 Hz, 1H). anti-(Z)-**45**, anti-(E)-**45** were known compound [44].

4.5.4. (E)-1,4-Diphenyl-2-ethyl-but-3-en-1-ol (**46**)

46 and **47** were isolated as an inseparable mixture (64.8 mg, 52%, yellow oil, R_f 0.40 and 0.38: EtOAc/hexane = 1:4).

major isomer: ^1H NMR (CDCl_3 , 400 MHz) δ 7.40–7.20 (m, 10H), 6.37 (d, $J = 15.6$ Hz, 1H), 5.89 (dd, $J = 9.6$, 16.0 Hz, 1H), 4.73 (t, $J = 5.2$ Hz, 1H), 2.49 (ddt, $J = 4.4$, 5.6, 9.6 Hz, 1H), 2.06 (br s, 1H), 1.42–1.22 (m, 2H), 0.90 (t, $J = 7.6$ Hz, 3H); ^{13}C NMR (CDCl_3 , 100 MHz) δ 142.6, 137.5, 132.7, 130.2, 128.6, 128.2, 127.6, 127.3, 126.8, 77.2, 52.6, 23.3, 12.2.

minor isomer: ^1H NMR (CDCl_3 , 400 MHz) δ 7.40–7.20 (m, 10H),

6.53 (d, $J = 16.0$ Hz, 1H), 6.06 (dd, $J = 9.2, 16.0$ Hz, 1H), 4.51 (dd, $J = 2.4, 8.0$ Hz, 1H), 2.37 (ddm, $J = 4.4, 9.6$ Hz, 1H), 2.17 (br s, 1H), 1.69 (dm, $J = 7.6$ Hz, 2H), 0.83 (t, $J = 7.6$ Hz, 3H); ^{13}C NMR (CDCl_3 , 100 MHz) δ 142.7, 137.2, 134.1, 130.7, 128.7, 128.4, 128.1, 127.8, 127.1, 126.4, 77.3, 54.0, 24.1, 12.1.

4.5.5. 1,2-Diphenylhex-3-en-1-ol (**47**)

The ^1H NMR spectrum of syn-(E)-**47** was identical with that reported in the literature [66].

Characteristic peaks of syn-(E)-**47**: ^1H NMR (CDCl_3 , 400 MHz) δ 5.56–5.46 (m, 1H), 5.31–5.22 (m, 1H), 4.85 (dd, $J = 3.2, 8.0$ Hz, 1H), 3.55 (t, $J = 8.0$ Hz, 1H), 1.95 (d, $J = 3.2$ Hz, 1H), 0.80 (t, $J = 7.6$ Hz, 3H).

Characteristic peaks of syn-(Z)-**47**: ^1H NMR (CDCl_3 , 400 MHz) δ 5.56–5.46 (m, 1H), 5.31–5.22 (m, 1H), 4.82 (dd, $J = 3.2, 9.2$ Hz, 1H), 3.89 (t, $J = 9.2$ Hz, 1H), 1.92 (d, $J = 3.2$ Hz, 1H), 0.63 (t, $J = 7.6$ Hz, 3H).

anti-(E)-**47** and anti-(Z)-**47** were known compounds [67].

4.5.6. (E)-1-(4-Methoxyphenyl)-2,4-diphenylbut-3-en-1-ol (**50**)

syn-**50** and anti-**50** were isolated as an inseparable mixture (116.9 mg, 71%, yellow oil, R_f 0.38: EtOAc/hexane = 3:7). The ^1H NMR spectrum of anti-**50** was identical with that reported in the literature [68]. anti-isomer: ^1H NMR (CDCl_3 , 400 MHz) δ 7.38–7.08 (m, 12H), 6.74 (dm, $J = 8.8$ Hz, 2H), 6.61 (dd, $J = 8.8, 16.0$ Hz, 1H), 6.53 (d, $J = 16.0$ Hz, 1H), 4.88 (dd, $J = 2.4, 8.0, 1H$), 3.73 (s, 3H), 3.68 (t, $J = 8.0$ Hz, 1H), 2.28 (d, $J = 2.4$ Hz, 1H); ^{13}C NMR (CDCl_3 , 100 MHz) δ 158.9, 141.0, 137.1, 134.19, 133.3, 129.5, 128.6, 128.5 (two peaks), 127.9, 127.6, 126.7, 126.4, 113.7, 77.3, 58.5, 55.2.

syn-isomer: ^1H NMR (CDCl_3 , 400 MHz) δ 7.38–7.08 (m, 12H), 6.85 (dm, $J = 8.8$ Hz, 2H), 6.25 (dd, $J = 8.0, 16.0$ Hz, 1H), 6.17 (d, $J = 16.0$ Hz, 1H), 4.93 (dd, $J = 2.4, 8.0$ Hz, 1H), 3.78 (s, 3H), 3.75 (t, $J = 8.0$ Hz, 1H), 1.95 (d, $J = 2.4$ Hz, 1H); ^{13}C NMR (CDCl_3 , 100 MHz) δ 159.2, 140.7, 137.3, 134.18, 132.2, 129.7, 128.94, 128.90, 128.5, 128.2, 127.3, 127.2, 126.2, 113.4, 77.4, 57.8, 55.3.

4.5.7. (E)-1-(2-Methoxyphenyl)-2,4-diphenylbut-3-en-1-ol (**51**)

syn-**51** and anti-**51** were isolated as an inseparable mixture (140.4 mg, 85%, yellow oil, R_f 0.38: EtOAc/hexane = 3:7). The ^1H NMR spectrum of anti-**51** was identical with that reported in the literature [68]. anti-isomer: ^1H NMR (CDCl_3 , 400 MHz) δ 7.41–7.10 (m, 12H), 6.92 (t, $J = 7.6$ Hz, 1H), 6.84 (d, $J = 7.6$ Hz, 1H), 6.60 (dd, $J = 8.4, 16.0$ Hz, 1H), 6.39 (d, $J = 16.0$ Hz, 1H), 5.23 (t, $J = 6.0$ Hz, 1H), 3.91 (t, $J = 6.0$ Hz, 1H), 3.77 (s, 3H), 2.72 ($J = 6.0$ Hz, 1H); ^{13}C NMR (CDCl_3 , 100 MHz) δ 156.5, 142.0, 137.5, 132.5, 130.3, 129.6, 128.47, 128.4, 128.2, 128.0, 127.2, 126.7, 126.3, 120.6, 110.4, 74.5, 55.8, 55.3.

syn-isomer: ^1H NMR (CDCl_3 , 400 MHz) δ 7.41–7.10 (m, 12H), 6.85 (t, $J = 7.6$ Hz, 1H), 6.70 (d, $J = 7.6$ Hz, 1H), 6.4 0 (dd, $J = 8.4, 16.0$ Hz, 1H), 6.19 (d, $J = 16.0$ Hz, 1H), 5.33 (dd, $J = 6.0, 8.4$ Hz, 1H), 3.84 (t, $J = 8.4$ Hz, 1H), 3.75 (s, 1H), 2.52 (d, $J = 6.0$ Hz, 1H); ^{13}C NMR (CDCl_3 , 100 MHz) δ 156.3, 141.1, 137.5, 131.1, 130.5, 128.8, 128.47 (two peaks), 128.3, 127.8, 127.0, 126.4, 126.1, 120.4, 110.3, 73.4, 57.0, 55.2.

4.5.8. (E)-1-(3,4-Methylenedioxyphenyl)-2,4-diphenylbut-3-en-1-ol (**52**)

syn-**52** and anti-**52** were isolated as an inseparable mixture (128.2 mg, 75%, yellow oil, R_f 0.30: EtOAc/hexane = 3:7). The ^1H NMR spectrum of anti-**52** was identical with that reported in the literature [68]. anti-isomer: ^1H NMR (CDCl_3 , 400 MHz) δ 7.38–7.10 (m, 10H), 6.75 (d, $J = 2.0$ Hz, 1H), 6.58 (dd, $J = 8.0, 16.0$ Hz, 1H), 6.60 (d, $J = 8.0$ Hz, 1H), 6.56 (dd, $J = 2.0, 8.0$ Hz, 1H), 6.52 (d, $J = 16.0$ Hz, 1H), 5.86 (dd, $J = 2.0, 4.8$ Hz, 2H), 4.82 (d, $J = 8.0$ Hz, 1H), 3.64 (t, $J = 8.0$ Hz, 1H), 2.33 (s, 1H); ^{13}C NMR (CDCl_3 , 100 MHz) δ 147.5, 146.8, 140.9, 137.0, 136.0, 133.5, 129.3, 128.6, 128.5, 128.4, 127.6, 126.7, 126.4, 120.4, 107.7, 107.1, 100.9, 58.5.

syn-isomer: ^1H NMR (CDCl_3 , 400 MHz) δ 7.38–7.10 (m, 10H), 6.85 (br s, 1H), 6.74 (dd, $J = 2.0, 8.0$ Hz, 1H), 6.72 (d, $J = 8.0$ Hz, 1H),

6.24 (dd, $J = 8.0, 16.0$ Hz, 1H), 6.17 (d, $J = 16.0$ Hz, 1H), 5.93 (d, $J = 1.6$ Hz, 1H), 5.92 (d, $J = 1.6$ Hz, 1H), 4.88 (d, $J = 8.0$ Hz, 1H), 3.71 (t, $J = 8.0$ Hz, 1H), 1.97 (s, 1H); ^{13}C NMR (CDCl_3 , 100 MHz) δ 147.8, 147.2, 140.6, 137.3, 136.0, 132.2, 129.5, 128.9, 128.8, 128.5, 127.3, 127.2, 126.2, 120.7, 107.9, 107.9, 107.1, 77.5, 57.8.

4.5.9. (E)-1-(4-Methoxycarbonylphenyl)-2,4-diphenylbut-3-en-1-ol (**53**)

syn-**53** and anti-**53** were isolated as an inseparable mixture (145.8 mg, 82%, colorless solid, R_f 0.35: EtOAc/hexane = 3:7). The ^1H NMR spectrum of anti-**53** was identical with that reported in the literature [68]. anti-isomer: ^1H NMR (CDCl_3 , 400 MHz) δ 7.89 (d, $J = 7.9$ Hz, 2H), 7.39–7.11 (m, 12H), 6.61 (dd, $J = 7.9, 15.8$ Hz, 1H), 6.53 (d, $J = 15.8$ Hz, 1H), 4.97 (dd, $J = 2.4, 7.9$ Hz, 1H), 3.88 (s, 3H), 3.68 (t, $J = 7.9$ Hz, 1H), 2.58 (d, $J = 2.4$ Hz, 1H); ^{13}C NMR (CDCl_3 , 100 MHz) δ 167.0, 147.2, 140.4, 136.8, 133.8 (two peaks), 129.3, 129.2, 128.8, 128.5, 128.4, 127.7, 127.0, 126.4, 126.2, 77.3, 58.4, 52.1.

syn-isomer: ^1H NMR (CDCl_3 , 400 MHz) δ 7.98 (d, $J = 7.9$ Hz, 2H), 7.39–7.11 (m, 12H), 6.30 (dd, $J = 7.9, 15.8$ Hz, 1H), 6.22 (d, $J = 15.8$ Hz, 1H), 5.05 (dd, $J = 3.2, 7.9$ Hz, 1H), 3.90 (s, 3H), 3.77 (t, $J = 7.9$ Hz, 1H), 2.27 (d, $J = 3.2$ Hz, 1H); ^{13}C NMR (CDCl_3 , 100 MHz) δ 167.0, 147.2, 139.9, 137.0, 132.6 (two peaks), 128.9, 128.6, 128.5, 127.5, 127.3, 127.0, 126.7, 77.4, 57.7, 52.1.

4.5.10. (E)-1-(4-Cyanophenyl)-2,4-diphenylbut-3-en-1-ol (**54**)

syn-**54** and anti-**54** were isolated as an inseparable mixture (87.7 mg, 54%, yellow solid, R_f 0.45: EtOAc/hexane = 3:7). The ^1H NMR spectrum of anti-**54** was identical with that reported in the literature [68]. anti-isomer: ^1H NMR (CDCl_3 , 400 MHz) δ 7.47 (d, $J = 8.8$ Hz, 2H), 7.38–7.17 (m, 10H), 7.09 (d, $J = 7.2$ Hz, 2H), 6.57 (dd, $J = 7.2, 15.6$ Hz, 1H), 6.52 (d, $J = 15.6$ Hz, 1H), 4.95 (d, $J = 7.2$ Hz, 1H), 3.61 (t, $J = 7.2$ Hz, 1H), 2.50 (s, 1H); ^{13}C NMR (CDCl_3 , 100 MHz) δ 147.4, 140.0, 136.6, 134.4, 131.9 (two peaks), 128.86, 128.3, 128.0, 127.5, 127.3, 126.5, 119.0, 111.3, 77.16, 58.7.

syn-isomer: ^1H NMR (CDCl_3 , 400 MHz) δ 7.57 (d, $J = 8.0$ Hz, 2H), 7.38–7.17 (m, 12H), 6.27 (dd, $J = 8.0, 15.6$ Hz, 1H), 6.19 (d, $J = 15.6$ Hz, 1H), 5.04 (dd, $J = 2.4, 8.0$ Hz, 1H), 3.70 (t, $J = 8.0$ Hz, 1H), 2.15 (d, $J = 2.4$ Hz, 1H); ^{13}C NMR (CDCl_3 , 100 MHz) δ 147.3, 139.4, 136.8, 133.1, 132.0 (two peaks), 129.1, 128.8, 128.6, 128.3, 127.7, 127.6, 126.3, 118.9, 111.5, 77.1, 58.0.

4.5.11. (E)-1-(4-Chlorophenyl)-2,4-diphenylbut-3-en-1-ol (**55**)

syn-**55** and anti-**55** were isolated as an inseparable mixture (119.1 mg, 72%, colorless solid, R_f 0.42: EtOAc/hexane = 3:7). The ^1H NMR spectrum of anti-**55** was identical with that reported in the literature [68]. anti-isomer: ^1H NMR (CDCl_3 , 400 MHz) δ 7.38–7.06 (m, 14H), 6.58 (dd, $J = 8.0, 16.0$ Hz, 1H), 6.52 (d, $J = 16.0$ Hz, 1H), 4.88 (d, $J = 8.0$ Hz, 1H), 3.62 (t, $J = 8.0$ Hz, 1H), 2.05 (s, 1H); ^{13}C NMR (CDCl_3 , 100 MHz) δ 140.5, 140.4, 136.8, 133.8 (two peaks), 133.1, 128.9, 128.7, 128.4, 128.2, 128.1, 127.8, 126.9, 126.5, 77.3, 58.6.

syn-isomer: ^1H NMR (CDCl_3 , 400 MHz) δ 7.38–7.06 (m, 14H), 6.25 (dd, $J = 8.0, 16.0$ Hz, 1H), 6.18 (d, $J = 16.0$ Hz, 1H), 4.95 (d, $J = 8.0$ Hz, 1H), 3.71 (t, $J = 8.0$ Hz, 1H), 2.03 (s, 1H); ^{13}C NMR (CDCl_3 , 100 MHz) δ 140.4, 140.0, 137.0, 133.5, 132.7 (two peaks), 129.0, 128.8, 128.7, 128.6, 128.4, 127.5, 127.4, 126.3, 77.2, 57.8.

4.5.12. (E)-1-(3-Furyl)-2,4-diphenylbut-3-en-1-ol (**57**)

syn-**57** and anti-**57** were isolated as an inseparable mixture (62.8 mg, 44%, yellow solid, R_f 0.38: EtOAc/hexane = 3:7). The ^1H NMR spectrum of anti-**57** was identical with that reported in the literature [68]. anti-isomer: ^1H NMR (CDCl_3 , 400 MHz) δ 7.39–7.17 (m, 12H), 6.59 (dd, $J = 4.4, 16.4$ Hz, 1H), 6.54 (d, $J = 16.4$ Hz, 1H), 6.18 (s, 1H), 4.95 (dd, $J = 3.6, 7.6$ Hz, 1H), 3.68 (quint, $J = 3.6$ Hz, 1H), 2.19 (d, $J = 3.6$ Hz, 1H); ^{13}C NMR (CDCl_3 , 100 MHz) δ 142.9, 141.0, 139.9, 137.0, 133.6, 129.3, 128.71, 128.7, 128.5, 127.7, 127.0, 126.7, 126.5,

109.0, 70.6, 57.5.

syn-isomer: ^1H NMR (CDCl_3 , 400 MHz) δ 7.39–7.17 (m, 12H), 6.36 (dd, $J = 5.2, 16.0$ Hz, 1H), 6.34 (s, 1H), 6.32 (dd, $J = 5.2, 16.0$ Hz, 1H), 5.01 (dd, $J = 3.6, 8.0$ Hz, 1H), 3.77 (quint, $J = 3.6$ Hz, 1H), 1.88 (d, $J = 3.6$ Hz, 1H); ^{13}C NMR (CDCl_3 , 100 MHz) δ 143.2, 140.4, 140.1, 137.2, 132.7, 129.2, 128.9, 128.8, 128.6, 127.5, 127.3, 126.6, 126.3, 109.1, 70.4, 56.7.

4.5.13. (*E*)-1,4,6-Triphenylhexa-1,5-dien-3-ol (**58**)

major isomer: ^1H NMR (CDCl_3 , 400 MHz) δ 7.42–7.18 (m, 15H), 6.66 (d, $J = 16.0$ Hz, 1H), 6.54–6.45 (m, 2H), 6.30 (dd, $J = 6.4, 16.0$ Hz, 1H), 4.66 (t, $J = 6.4$ Hz, 1H), 3.70 (dt, $J = 3.6, 6.4$ Hz, 1H); ^{13}C NMR (CDCl_3 , 100 MHz) δ 140.5, 137.2, 136.8, 132.9, 131.8, 129.9, 129.2, 129.0, 128.8, 128.7, 128.6, 127.8, 127.6, 127.2, 126.7, 126.4, 75.7, 56.6; HRMS (EI): found 308.1565. $\text{C}_{24}\text{H}_{20}$ ($-\text{H}_2\text{O}$) requires 308.1580.

minor isomer: ^1H NMR (CDCl_3 , 400 MHz) δ 7.42–7.18 (m, 15H), 6.63–6.55 (m, 3H), 6.15 (dd, $J = 6.4, 16.0$ Hz, 1H), 4.61 (dt, $J = 1.2, 6.4$ Hz, 1H), 3.64 (m, 1H); Characteristic peaks of ^{13}C NMR (CDCl_3 , 100 MHz) δ 140.9, 137.1, 136.9, 132.9, 131.4, 129.3, 128.8, 128.6, 127.8, 127.7, 127.1, 126.6, 126.5, 75.6, 56.9.

4.5.14. (*E*)-1,3-Diphenyl-5-methylhex-1-en-4-ol (**59**)

The ^1H NMR spectrum of anti-**59** was identical with that reported in the literature [68].

anti-isomer: ^1H NMR (CDCl_3 , 400 MHz) δ 7.41–7.18 (m, 10H), 6.59–6.53 (m, 2H), 3.68 (dd, $J = 4.8, 7.2$ Hz, 1H), 3.60–3.56 (m, 1H), 1.89 (m, 1H), 1.55 (br s, 1H), 1.06 (d, $J = 7.2$ Hz, 3H), 0.99 (d, $J = 7.2$ Hz, 3H); ^{13}C NMR (CDCl_3 , 100 MHz) δ 142.3, 137.2, 132.8, 130.0, 128.9, 128.7, 128.1, 127.6, 126.8, 126.4, 79.2, 53.8, 30.1, 20.2, 16.2.

syn-isomer: ^1H NMR (CDCl_3 , 400 MHz) δ 7.41–7.18 (m, 10H), 6.47 (d, $J = 16.0$ Hz, 1H), 6.39 (dd, $J = 8.0, 16.0$ Hz, 1H), 3.80 (dd, $J = 3.6, 8.4$ Hz, 1H), 3.60–3.56 (m, 1H), 1.67 (m, 1H), 1.55 (br s, 1H), 0.99 (d, $J = 7.2$ Hz, 3H), 0.95 (d, $J = 6.8$ Hz, 3H); ^{13}C NMR (CDCl_3 , 100 MHz) δ 141.6, 137.4, 131.2, 130.7, 129.0, 128.7, 127.5, 127.1, 126.3, 78.9, 54.2, 30.4, 20.6, 15.1.

4.5.15. (*E*)-1-Phenyl-2,4-di(4-methoxyphenyl)but-3-en-1-ol (**61**)

syn-**61** and anti-**61** were isolated as an inseparable mixture (1.038 g, 72%, colorless solid, R_f 0.42: EtOAc/hexane = 3:7).

anti-isomer: ^1H NMR (CDCl_3 , 400 MHz) δ 7.32–7.10 (m, 8H), 7.03–6.99 (m, 1H), 6.90–6.87 (m, 1H), 6.84–6.82 (m, 1H), 6.78–6.73 (m, 2H), 6.46 (d, $J = 16.0$ Hz, 1H), 6.41 (dd, $J = 8.0, 16.0$ Hz, 1H), 4.85 (d, $J = 8.0$ Hz, 1H), 3.75 (s, 3H), 3.73 (s, 3H), 3.64 (t, $J = 8.0$ Hz, 1H), 2.37 (s, 1H); ^{13}C NMR (CDCl_3 , 100 MHz) δ 159.3, 158.3, 142.2, 133.2, 132.8, 130.0, 129.4, 128.1, 127.6, 127.5, 127.2, 126.9, 114.1, 113.9, 77.9, 57.6, 55.4, 55.3.

anti-**61** was prepared according to the reported method [68]. The ^1H and ^{13}C NMR data are in good agreement with each other.

syn-isomer: ^1H NMR (CDCl_3 , 400 MHz) δ 7.32–7.10 (m, 8H), 7.03–6.99 (m, 1H), 6.90–6.87 (m, 1H), 6.84–6.82 (m, 1H), 6.78–6.73 (m, 2H), 6.12 (d, $J = 16.0$ Hz, 1H), 6.09 (dd, $J = 4.0, 16.0$ Hz, 1H), 4.91 (dd, $J = 1.2, 8.0$ Hz, 1H), 3.80 (s, 3H), 3.71 (dd, $J = 4.0, 8.0$ Hz, 1H), 2.04 (s, 1H); ^{13}C NMR (CDCl_3 , 100 MHz) δ 159.1, 158.8, 142.2, 132.8, 132.5, 131.6 (two peaks), 130.2, 128.2, 127.8, 127.42, 127.1, 114.3, 114.0, 78.0, 56.9, 55.4, 55.4 (two peaks).

Declaration of competing interest

The authors declare that they have no known competing financial interests or personal relationships that could have appeared to influence the work reported in this paper.

Acknowledgments

We thank Mr. Yuhei Hayashi (University of Toyama) for checking

some reactions for reproducibility. This work was financially supported by JSPS KAKENHI Grant Number JP18K05101.

Appendix A. Supplementary data

Supplementary data to this article can be found online at <https://doi.org/10.1016/j.tet.2020.131493>.

Supplementary Material

Supplementary material that may be helpful in the review process should be prepared and provided as a separate electronic file. That file can then be transformed into PDF format and submitted along with the manuscript and graphic files to the appropriate editorial office.

References

- [1] S.E. Denmark, G.L. Beutner, *Angew. Chem. Int. Ed.* 47 (2008) 1560–1638.
- [2] C. Chuit, R.J.P. Corriu, C. Reye, J.C. Young, *Chem. Rev.* 93 (1993) 1371–1448.
- [3] L. Chabaud, P. James, Y. Landais, *Eur. J. Org. Chem.* (2004) 3173–3199.
- [4] T. Komiyama, Y. Minami, T. Hiyama, *ACS Catal.* 7 (2017) 631–651.
- [5] Y. Hatanaka, T. Hiyama, *J. Org. Chem.* 53 (1988) 918–920.
- [6] T. Hiyama, Y. Hatanaka, *Pure Appl. Chem.* 66 (1994) 1471–1478.
- [7] T. Komiyama, Y. Minami, T. Hiyama, *Synlett* 28 (2017) 1873–1884.
- [8] A. Hosomi, M. Endo, H. Sakurai, *Chem. Lett.* 5 (1976) 941–942.
- [9] A. Hosomi, H. Sakurai, *Tetrahedron Lett.* 17 (1976) 1295–1298.
- [10] A. Hosomi, H. Sakurai, *J. Am. Chem. Soc.* 99 (1977) 1673–1675.
- [11] S.E. Denmark, *J. Fu. Chem. Rev.* 103 (2003) 2763–2794.
- [12] M. Wadamoto, H. Yamamoto, *J. Am. Chem. Soc.* 127 (2005) 14556–14557.
- [13] C.H. Larsen, B.H. Ridgway, J.T. Shaw, D.M. Smith, K.A. Woerpel, *J. Am. Chem. Soc.* 127 (2005) 10879–10884.
- [14] J.L. Hofstra, A.H. Cherney, C.M. Ordner, S.E. Reisman, *J. Am. Chem. Soc.* 140 (2018) 139–142.
- [15] C. Luo, J.S. Bandar, *J. Am. Chem. Soc.* 141 (2019) 14120–14125.
- [16] B.M. Trost, D.L. Van Vranken, *Chem. Rev.* 96 (1996) 395–422.
- [17] J.D. Weaver, A. Recio, A.J. Grenning, J.A. Tunge, *Chem. Rev.* 111 (2011) 1846–1913.
- [18] A.S. Pilcher, H.L. Ammon, P. DeShong, *J. Am. Chem. Soc.* 117 (1995) 5166–5167.
- [19] É. Bélanger, K. Cantin, O. Messe, M. Tremblay, J.F. Paquin, *J. Am. Chem. Soc.* 129 (2007) 1034–1035.
- [20] A.S. Pilcher, P. DeShong, *J. Org. Chem.* 61 (1996) 6901–6905.
- [21] M.-R. Brescia, P. DeShong, *J. Org. Chem.* 63 (1998) 3156–3157.
- [22] C.J. Handy, Y.F. Lam, P. DeShong, *J. Org. Chem.* 65 (2000) 3542–3543.
- [23] M.E. Hoke, M.-R. Brescia, S. Bogaczyk, P. DeShong, B.W. King, M.T. Crimmins, *J. Org. Chem.* 67 (2002) 327–335.
- [24] M.H. Katcher, A.G. Doyle, *J. Am. Chem. Soc.* 132 (2010) 17402–17404.
- [25] Philip L. Fuchs, *Handbook of Reagents for Organic Synthesis, Reagents for Silicon-Mediated Organic Synthesis*, 2011.
- [26] Y. Horino, N. Homura, K. Inoue, S. Yoshikawa, *Adv. Synth. Catal.* 354 (2012) 828–834.
- [27] Y. Horino, Y. Takahashi, K. Koketsu, H. Abe, K. Tsuge, *Org. Lett.* 16 (2014) 3184–3187.
- [28] J.D. Buynak, J.B. Strickland, G.W. Lamb, D. Khasnis, S. Modi, D. Williams, H. Zhang, *J. Org. Chem.* 56 (1991) 7076–7083.
- [29] K. Tatsumi, S. Tanabe, Y. Tsuji, T. Fujihara, *Org. Lett.* 21 (2019) 10130–10133.
- [30] L.J. Cheng, N.P. Mankad, *J. Am. Chem. Soc.* 142 (2020) 80–84.
- [31] B.M. Trost, Z.T. Ball, *J. Am. Chem. Soc.* 126 (2004) 13942–13944.
- [32] B.M. Trost, A. Bertogg, *Org. Lett.* 11 (2009) 511–513.
- [33] K. Okamoto, E. Tamura, K. Ohe, *Angew. Chem. Int. Ed.* 52 (2013) 10639–10643.
- [34] E. Fillion, R.J. Carson, V.E. Trépanier, J.M. Goll, A.A. Remorova, *J. Am. Chem. Soc.* 126 (2004) 15354–15355.
- [35] E. Fillion, V.E. Trépanier, J.J. Heikkinen, A.A. Remorova, R.J. Carson, J.M. Goll, A. Seed, *Organometallics* 28 (2009) 3518–3531.
- [36] T. Korenaga, A. Ko, K. Uotani, Y. Tanaka, T. Sakai, *Angew. Chem. Int. Ed.* 50 (2011) 10703–10707.
- [37] T. Korenaga, R. Sasaki, K. Shimada, *Dalton Trans.* 44 (2015) 19642–19650.
- [38] V. Corcé, L.M. Chamoreau, E. Derat, J.P. Goddard, C. Ollivier, L. Fensterbank, *Angew. Chem. Int. Ed.* 54 (2015) 11414–11418.
- [39] We Thank an Anonymous Reviewer for Providing Insightful Comments and Suggestions.
- [40] Gaussian 16, Revision C. 01, M.J. Frisch, G.W. Trucks, H.B. Schlegel, G.E. Scuseria, M.A. Robb, J.R. Cheeseman, G. Scalmani, V. Barone, G.A. Petersson, H. Nakatsuji, X. Li, M. Caricato, A.V. Marenich, J. Bloino, B.G. Janesko, R. Gomperts, B. Mennucci, H.P. Hratchian, J.V. Ortiz, A.F. Izmaylov, J.L. Sonnenberg, D. Williams-Young, F. Ding, F. Lipparini, F. Egidi, J. Goings, B. Peng, A. Petrone, T. Henderson, D. Ranasinghe,

- V.G. Zakrzewski, J. Gao, N. Rega, G. Zheng, W. Liang, M. Hada, M. Ehara, K. Toyota, R. Fukuda, J. Hasegawa, M. Ishida, T. Nakajima, Y. Honda, O. Kitao, H. Nakai, T. Vreven, K. Throssell, J.A. Montgomery Jr., J.E. Peralta, F. Ogliaro, M.J. Bearpark, J.J. Heyd, E.N. Brothers, K.N. Kudin, V.N. Staroverov, T.A. Keith, R. Kobayashi, J. Normand, K. Raghavachari, A.P. Rendell, J.C. Burant, S.S. Iyengar, J. Tomasi, M. Cossi, J.M. Millam, M. Klene, C. Adamo, R. Cammi, J.W. Ochterski, R.L. Martin, K. Morokuma, O. Farkas, J.B. Foresman, D.J. Fox, Gaussian, Inc., Wallingford CT, 2019.
- [41] Since the IRC Calculation for the Transition-State of Oxidative Addition (TS³⁴⁻³⁵) Did Not Proceed, the Transition-State Was Confirmed by the NEB Method Using Reaction Plus Pro2 Software.
- [42] A. Hosomi, A. Shirahata, H. Sakurai, Chem. Lett. 7 (1978) 901–904.
- [43] A. Hosomi, A. Shirahata, H. Sakurai, Tetrahedron Lett. 19 (1978) 3043–3046.
- [44] T. Hayashi, Y. Matsumoto, T. Kiyoi, Y. Ito, S. Kohra, Y. Tominaga, A. Hosomi, Tetrahedron Lett. 29 (1988) 5667–5670.
- [45] S. Hayashi, K. Hirano, H. Yorimitsu, K. Oshima, J. Am. Chem. Soc. 128 (2006) 2210–2211.
- [46] J.F. Cívicos, D.A. Alonso, C. Nájera, Adv. Synth. Catal. 353 (2011) 1683–1687.
- [47] S. Zhang, Y. Wang, X. Feng, M. Bao, J. Am. Chem. Soc. 134 (2012) 5492–5495.
- [48] Y. Tsuji, S. Kajita, S. Isobe, M. Funato, J. Org. Chem. 58 (1993) 3607–3608.
- [49] K. Nakajima, X. Guo, Y. Nishibayashi, Chem. Asian J. 13 (2018) 3653–3657.
- [50] G. Wang, Y. Gan, Y. Liu, Chin. J. Chem. 36 (2018) 916–920.
- [51] M. Sai, Adv. Synth. Catal. 360 (2018) 3482–3487.
- [52] B. Yang, Z.-X. Wang, J. Org. Chem. 82 (2017) 4542–4549.
- [53] X.-L. Tang, Z. Wu, M.-B. Li, Y. Gu, S.-K. Tian, Eur. J. Org. Chem. (2012) 4107–4109.
- [54] P.-A. Deyris, T. Cañeque, Y. Wang, P. Retailleau, F. Bigi, R. Maggi, G. Maestri, M. Malacria, ChemCatChem 7 (2015) 3266–3269.
- [55] S.-R. Sheng, X. Huang, J. Chin. Chem. Soc. 50 (2003) 893–896.
- [56] C. Chen, T.R. Dugan, W.W. Brennessel, D.J. Weix, P.L. Holland, J. Am. Chem. Soc. 136 (2014) 945–955.
- [57] R. Riveiros, R. Tato, J. Pérez Sestelo, L.A. Sarandeses, Eur. J. Org. Chem. (2012) 3018–3023.
- [58] G. Li, L. Wu, G. Lv, H. Liu, Q. Fu, X. Zhang, Z. Tang, Chem. Commun. 50 (2014) 6246–6248.
- [59] J. Kuroda, K. Inamoto, K. Hiroya, T. Doi, Eur. J. Org. Chem. (2009) 2251–2261.
- [60] D. Heijnen, F. Tosi, C. Vila, M.C.A. Stuart, P.H. Elsinga, W. Szymanski, B.L. Feringa, Angew. Chem. Int. Ed. 56 (2017).
- [61] M. Tobisu, T. Takahira, T. Morioka, N. Chatani, J. Am. Chem. Soc. 138 (2016) 6711–6714.
- [62] T. Satoh, N. Hanaki, N. Yamada, T. Asano, Tetrahedron 56 (2000) 6223–6234.
- [63] F. Ding, R. William, F. Wang, X.W. Liu, Chem. Commun. 48 (2012) 8709–8711.
- [64] F. Chen, Y. Chen, H. Cao, Q. Xu, L. Yu, J. Org. Chem. 83 (2018) 14158–14164.
- [65] Y. Horino, A. Aimono, H. Abe, Org. Lett. 17 (2015) 2824–2827.
- [66] E.S. Schmidtman, M. Oestreich, Angew. Chem. Int. Ed. 48 (2009) 4634–4638.
- [67] Y. Horino, M. Sugata, H. Abe, Adv. Synth. Catal. 358 (2016) 1023–1028.
- [68] Y. Horino, M. Sugata, I. Mutsuura, K. Tomohara, H. Abe, Org. Lett. 19 (2017) 5968–5971.